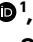



A root-based *N*-hydroxypipecolic acid standby circuit to direct immunity and growth of *Arabidopsis* shoots

Received: 15 November 2024

Accepted: 13 June 2025

Published online: 22 July 2025

 Check for updatesPing Xu¹ , Sophia Fundneider¹, Birgit Lange¹, Rafat Maksym¹, Johannes Stuttmann² & Anton R. Schäffner¹ ✉

Soil-borne microorganisms can systemically affect shoot resistance to pathogens relying on jasmonic acid and/or salicylic acid. However, the emanating root triggers in these scenarios remain elusive. Here we identify an *N*-hydroxypipecolic-acid-(NHP-)directed, salicylic-acid-related mechanism of root-triggered systemic resistance in *Arabidopsis*, which uses components of systemic acquired resistance known in leaves. However, in contrast to the inductive nature of systemic acquired resistance, FLAVIN-DEPENDENT MONOOXYGENASE 1 (FMO1) continuously synthesizes NHP in roots, while the glucosyltransferase UGT76B1 concomitantly conjugates and immobilizes NHP. Physical grafting experiments and tissue-specific knockouts revealed that the loss of UGT76B1 in roots leads to enhanced NHP release, initiating shoot responses. This counteracting standby FMO1/UGT76B1 circuit is specifically and sensitively modulated by root-associated microorganisms. Endophytic and (hemi)biotrophic fungi induce UGT76B1 degradation and FMO1 expression, resulting in varying levels of NHP being released to the shoot, where this root signal differently modulates defence and growth.

In addition to local responses to pathogens, pests or chemical agents, defence against future challenges can also be triggered in distant tissues. These systemically spreading phenomena rely on various mechanisms and are broadly subsumed in ‘induced systemic resistance’ as advocated by De Kesel et al.^{1–10}. Induced systemic resistance *sensu stricto* was originally coined to denote the enhanced shoot resistance triggered by the plant-growth-promoting rhizobacterium *Pseudomonas simiae* (former *fluorescens*) WCS417r, which was genetically dependent on jasmonic acid (JA) and ethylene (ET) responsiveness^{1,11}. Numerous phenotypically similar instances of induced resistance and/or growth promotion were attributed to other root-associated microorganisms, such as *Fusarium*, *Colletotrichum* and *Trichoderma* species. Interestingly, the enhanced shoot defence status could also involve pipecolic acid and salicylic acid (SA) signalling in leaves, in conjunction or antagonistically with the JA/ET pathway^{1,12–18}

(Supplementary Table 1). Furthermore, the impact of, for example, *Fusarium* and *Colletotrichum* strains on the root transcriptome has been assessed^{14,19–23} (Supplementary Table 1). However, the nature of the root signals triggering the shoot response remained elusive.

Systemic acquired resistance (SAR) is leaf-to-leaf induced systemic resistance enhancing the immune status in distant leaves upon a local infection. It is associated with enhanced expression of *PATHOGENESIS-RELATED* (PR) genes and largely depends on SA^{10,24–26}. FLAVIN-DEPENDENT MONOOXYGENASE 1 (FMO1) is induced in the primary infected leaves, catalysing the biosynthesis of *N*-hydroxypipecolic acid (NHP). Among other long-distance signals, the movement of NHP is essential to trigger SA-dependent SAR in distant, systemic leaves^{7,27–31}. The small-molecule glucosyltransferase UGT76B1 constitutes a negative regulator in this scenario. UGT76B1 is induced post infection to inactivate both NHP and SA via *O*-glucosylation and to

¹Institute of Biochemical Plant Pathology, Helmholtz Zentrum München, Neuherberg, Germany. ²CEA, CNRS, BIAM, UMR7265, LEMiRE (Rhizosphère et Interactions Sol-Plante-Microbiote), Aix Marseille University, Saint-Paul lez Durance, France. ✉e-mail: schaeffner.lab@gmail.com

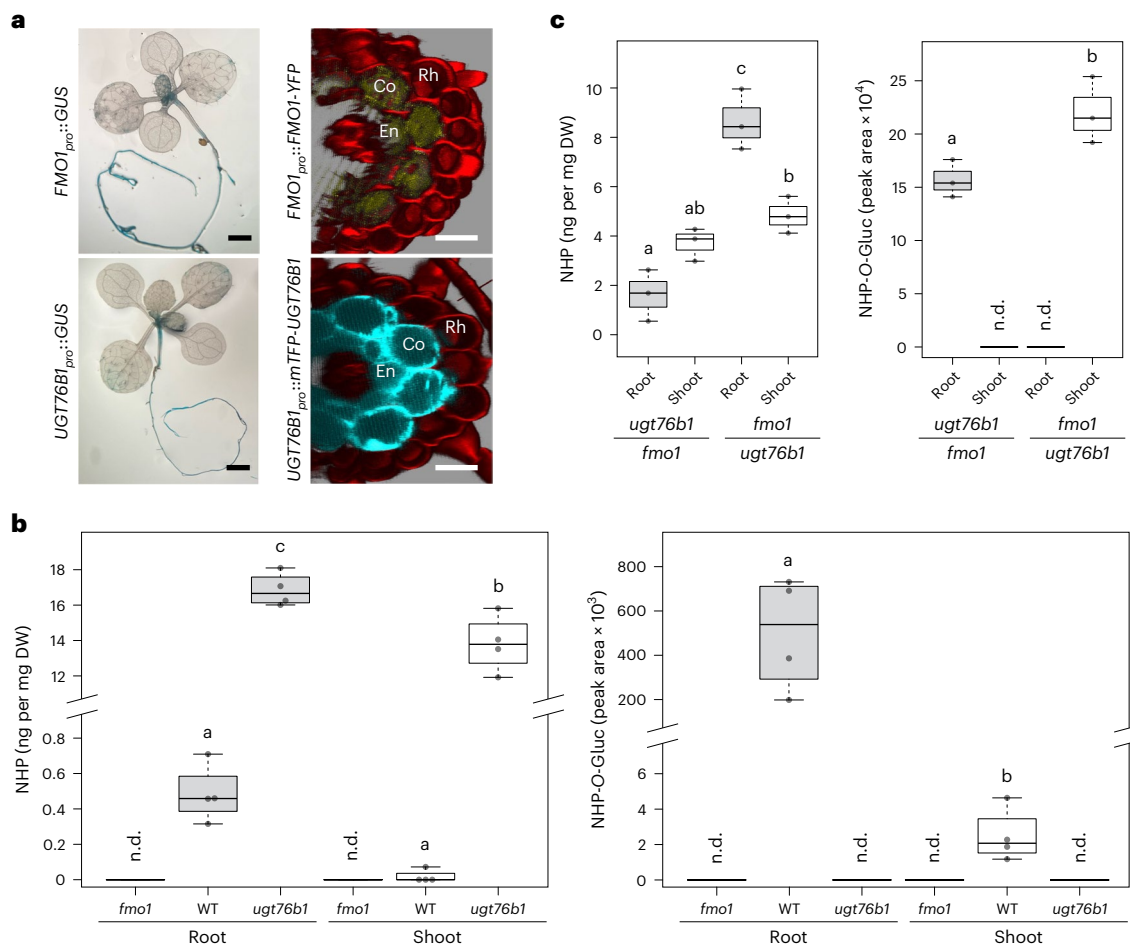


Fig. 1 | NHP biosynthesis and root–shoot mobility. a, Expression patterns of *UGT76B1* and *FMO1* transcripts and protein levels in 12-day-old naive plants grown on soil. Transcript levels were visualized via GUS staining using transgenic plants carrying *UGT76B1_{pro}::GFP-GUS* and *FMO1_{pro}::GUS* constructs (left). Protein levels were analysed via confocal laser scanning microscopy of main roots from two-week-old *ugt76b1* complemented with *UGT76B1_{pro}::mTFP-UGT76B1* and *fmo1* complemented with *FMO1_{pro}::FMO1-YFP* grown on half-strength Murashige and Skoog (MS) plates (right). Red indicates propidium iodide, yellow indicates FMO1-YFP and cyan indicates mTFP-UGT76B1. Scale bars, 3 mm (left) and 30 μ m (right). En, endodermis; Co, cortex; Rh, rhizodermis. The experiment was repeated three times with similar results. **b**, Levels of NHP and NHP-O-Gluc in root and shoot tissues of two-week-old plants grown on half-strength MS plates, determined via LC-MS analysis. $n = 4$. Significant differences between roots and shoots of different genotypes were analysed using two-way analysis of variance (ANOVA) with post hoc Tukey's test, as

indicated by the letters ($P_{adj} < 0.05$). Overall, metabolite levels correlate with FMO1 and UGT76B1 transcript and protein levels. WT metabolites were analysed three times, and the additional reference values of *ugt76b1* and *fmo1* organs were obtained once. DW, dry weight; n.d., not detectable. **c**, NHP-deficient *fmo1* shoots were grafted onto *ugt76b1* roots (incapable of NHP glucosylation), and vice versa. Roots and shoots of three-week-old grafted plants were sprayed with 1 mM BTH and separately harvested for LC-MS analysis after two days. NHP-O-Gluc was detected exclusively in tissues containing a functional UGT76B1 enzyme, demonstrating its immobility. The distribution of NHP in rosettes and roots in both grafting combinations highlights NHP's bidirectional mobility. $n = 3$. Root tissues are indicated in grey, shoot tissues in white. The boxes represent the interquartile range (IQR, Q1–Q3), with the median shown as a bold line. The whiskers extend to $1.5 \times$ IQR. The experiment was conducted twice with similar results.

attenuate defence. Accordingly, *fmo1* knockouts have compromised SAR²⁵, whereas the loss of UGT76B1 leads to the autonomous activation of SAR^{32–35}. It remains unclear whether SA-dependent shoot immunity triggered by root-associated microorganisms involves an analogous mechanism. Notably, UGT76B1 is constitutively expressed in the roots of naïve plants³⁶, and, given that root uptake of NHP can potentially trigger shoot defence^{37–39}, we reason that NHP could play a key role in mediating soil microbe–plant interactions and serve as a long-distance root-to-shoot signal.

Results

NHP is continuously synthesized and glucosylated in roots

The gene encoding the small-molecule glucosyltransferase UGT76B1 is induced in the shoot under stress conditions, where it glucosylates three defence-related compounds: isoleucic acid, SA and NHP^{33,36,40}.

However, its role in roots has remained unexplored, despite its constitutive expression in the root endodermis and cortex of naïve plants³⁶. To explore this expression pattern, we analysed the co-regulation between *UGT76B1* and the genes involved in the biosynthesis of its substrates. We focused on genes involved in SA and NHP biosynthesis, since the processes leading to isoleucic acid are elusive. Among these, *FMO1* (encoding the final step of NHP biosynthesis) shows the highest co-expression with *UGT76B1* (Supplementary Table 2). Promoter–GUS experiments indicate a high basal expression of *FMO1* and *UGT76B1* in the root^{36,41} (Fig. 1a). For a more detailed examination, we used transgenic lines expressing fluorescent-protein-labelled UGT76B1 and FMO1. mTFP-UGT76B1 is present in both the endodermis and cortex, whereas FMO1-YFP⁴² is detectable only in the cortex (Fig. 1a). Additionally, root single-cell expression data largely confirm that *FMO1* is permanently expressed in the cortex and differentiating

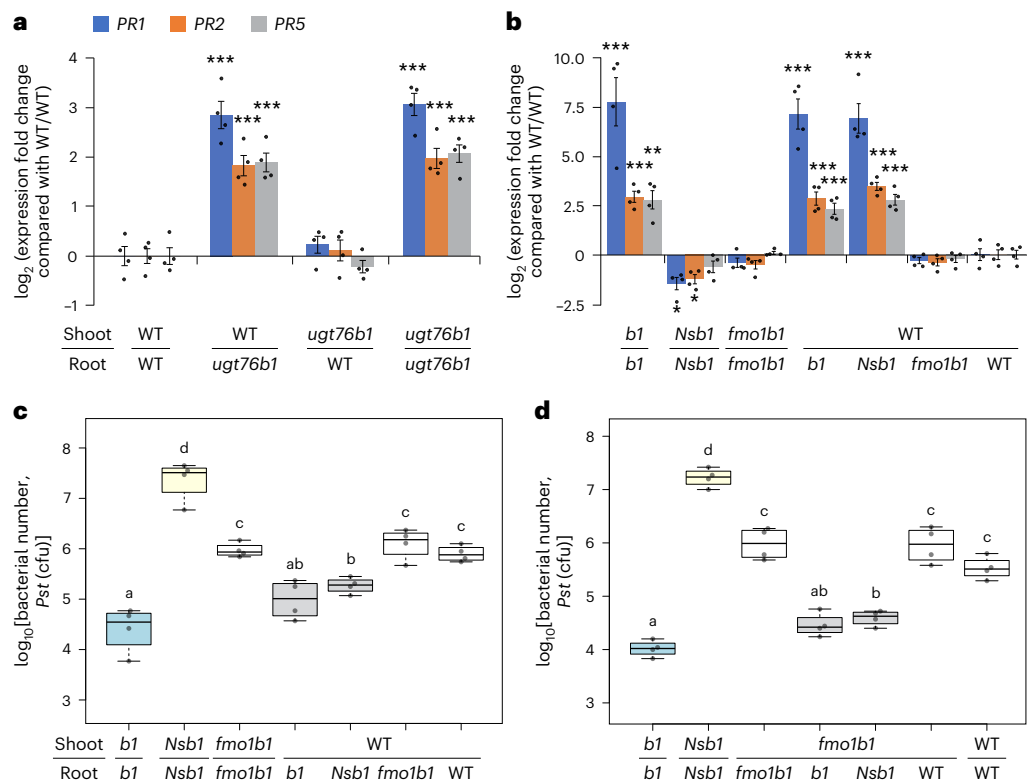


Fig. 2 | Impact of FMO1 and UGT76B1 root expression on shoot defence responses. a, b, Expression of SA-inducible defence genes *PR1*, *PR2* and *PR5* in shoots of grafted plants. The plants were grown under sterile conditions on half-strength MS plates. The bars represent means \pm standard error of the mean; $n = 4$. The absence of UGT76B1 in roots is associated with the upregulation of *PR* genes in shoots, an effect not observed when *ugt76b1* is knocked out only in shoots (**a**). Root-*ugt76b1*-dependent enhancement of SA signalling marker expression in shoots is abolished by the additional loss of FMO1 in roots but is unaffected by SA depletion in roots through the introduction of bacterial SA hydroxylase NahG and SA biosynthesis gene *sid2* knockout (**b**). *b1*, *ugt76b1*; *Nsb1*, NahG *sid2* *ugt76b1*. Data from reverse transcription-quantitative PCR are normalized to the WT/WT combination; *S16* and *UBQ5* are used as reference genes. **c**, *ugt76b1* and NahG *sid2* *ugt76b1* homografts serve as extremely resistant and susceptible references, respectively (shown in blue and yellow), for comparison with WT and

fmo1 *ugt76b1* homografts. Enhanced defence against *Pst* DC3000 is observed when UGT76B1 is absent in roots. However, this enhancement is lost when FMO1 is also absent in roots, whereas the absence of root-expressed SID2 and the ectopic expression of the SA hydroxylase NahG do not impact this enhancement of defence. **d**, Similar to the grafting combinations in **c**, here *fmo1* *ugt76b1* was used as the shoot in heterografts due to its inability to produce or *O*-glucosylate NHP. The enhanced resistance in these shoots is exclusively dependent on root-synthesized NHP. $n = 4$. The boxes represent the IQR (Q1–Q3), with the median shown as a bold line. The whiskers extend to $1.5 \times$ IQR. Significant differences between grafting combinations were analysed using the Welch two-sample *t*-test (* $P < 0.05$; ** $P < 0.01$; *** $P < 0.001$) for **a** and **b**, or one-way ANOVA with post hoc Tukey test for **c** and **d** (indicated by letters, $P_{\text{adj}} < 0.05$). All experiments (**a–d**) were repeated twice with similar results.

endodermis/cortex cells, whereas *UGT76B1* is strongly expressed in the endodermis, cortex and rhizodermis^{43,44} (Supplementary Fig. 1a,b). To detect products of both enzymes, we analysed extracts from roots and shoots using liquid chromatography–mass spectrometry (LC–MS). Consistent with the expression patterns, NHP and NHP-*O*-Gluc levels were notably higher in the roots than in the shoots of wild-type (WT) plants (Fig. 1b).

NHP but not NHP-*O*-Gluc is bidirectionally mobile between root and shoot

Although NHP is known to move systemically between leaves^{34,37}, its mobility between roots and shoots (as well as that of NHP-*O*-Gluc) remains unclear. To address this, reciprocal grafting was performed between *ugt76b1* and *fmo1*. Grafts between *ugt76b1*_{shoot} and *fmo1*_{root} enable NHP synthesis only in the shoot, with NHP *O*-glucosylation restricted to the root, and vice versa for *fmo1*_{shoot}/*ugt76b1*_{root} plants. Grafted plants were treated with benzothiadiazole (BTH) to induce NHP biosynthesis, and roots and shoots were separately collected for metabolic analysis. NHP-*O*-Gluc was detectable only in tissues expressing UGT76B1, indicating its immobility. In contrast, NHP was found in both roots and shoots even in the absence of FMO1, strongly suggesting that NHP moves bidirectionally between roots and shoots (Fig. 1c).

Lack of root expression of UGT76B1 induces shoot defence via NHP

To investigate the role of UGT76B1 in the root, we generated localized knockouts in roots or shoots using grafts combining WT plants and *ugt76b1*. After a 16-day recovery, shoots of three-week-old plants were harvested for expression analysis. Compared with WT control homografts, shoots of *ugt76b1* homografts showed strong upregulation of the SA-inducible defence genes *PR1*, *PR2* and *PR5*. The local loss of UGT76B1 in roots also promoted the expression of these *PR* genes in WT shoots, whereas the loss of UGT76B1 in shoots alone did not affect their expression (Fig. 2a).

To assess whether UGT76B1 substrates in the root affect shoot phenotypes, we combined SA- and NHP-defective mutations with *ugt76b1*. In homografts, the induction of *PR* genes was abolished when *fmo1* or NahG *sid2* were introgressed into *ugt76b1*. However, in heterografts, *ugt76b1* root-induced *PR* gene expression in WT shoots was retained when SA was depleted in the root but abolished when NHP was depleted by the loss of FMO1 (Fig. 2b and Extended Data Fig. 1).

Similarly, *ugt76b1* roots enhanced the resistance of WT shoots against *Pseudomonas syringae* DC3000 (*Pst*), reaching the level of *ugt76b1* homografts. In WT_{shoot}/NahG *sid2* *ugt76b1*_{root} plants, the depletion of SA in roots did not alter the enhanced shoot resistance caused

by the loss of UGT76B1 in roots, suggesting that root-derived SA does not influence shoot defence in this scenario. However, when FMO1 was eliminated in *ugt76b1* roots, the shoot resistance relapsed to WT levels (Fig. 2c). Due to the positive feedback loop of NHP biosynthesis⁴⁵, root-derived NHP may amplify its biosynthesis in the shoot. Additional grafting combinations using *fmo1 ugt76b1* as shoots were therefore tested for *Pst* resistance (Fig. 2d). As these shoots cannot synthesize or *O*-glucosylate NHP, their defence depends entirely on root-derived NHP. Consistently, root SA depletion did not impact the enhanced shoot defence induced by *ugt76b1* roots, whereas NHP depletion in roots abolished this effect. In conclusion, the enhanced defence of *ugt76b1* knockout plants results from NHP's presence in roots, where it is constitutively synthesized and transported to the shoot in the absence of a counteracting glucosylation capability.

UGT76B1 endodermal expression is critical for root-controlled shoot phenotypes

To investigate the role of UGT76B1 at the cell-layer level, we employed tissue-specific knockout (TSKO) to achieve 'genetic grafting'. We used a fluorescently labelled complementation line, *ugt76b1 UGT76B1_{pro}::mTFP-UGT76B1 (Compl.B1)*, as the parental line for TSKO, which allows visualizing and confirming the targeted knockout. An mCherry-labelled Cas9 protein was driven by the tissue-specific promoter *CO2* or *CASP1* to target *UGT76B1* in cortical or endodermal cells, respectively. In the endodermis-specific knockout line (*ugt76b1_{en}*), the mTFP-UGT76B1 signal was absent in endodermal cells. In the cortex-specific knockout line (*ugt76b1_{co}*), mTFP-UGT76B1 was eliminated in the cortex. Both knockouts were stable, with the targeted cell layers showing no mTFP signal (that is, UGT76B1 expression), even upon BTH induction of UGT76B1 (Fig. 3a and Extended Data Fig. 2).

Upon *Pst* infection, *Compl.B1* exhibited susceptibility similar to that of the WT, indicating successful complementation. The enhanced resistance of *ugt76b1_{en}* against *Pst* matched that of the full-knockout mutant, while *ugt76b1_{co}* exhibited intermediate resistance between the WT and *ugt76b1* (Fig. 3b and Extended Data Fig. 3). This enhanced resistance is consistent with the elevated NHP levels in both TSKO lines. However, unlike *ugt76b1*, both TSKO lines accumulated high levels of NHP-*O*-Gluc, as they retain intact UGT76B1 in the shoot (Fig. 3c). Additionally, *ugt76b1* plants showed slower growth, earlier senescence³⁶ and lower anthocyanin accumulation than the WT. *ugt76b1_{en}* mirrored these phenotypes, whereas *ugt76b1_{co}* was intermediate between the WT and *ugt76b1* (Extended Data Fig. 4a,b). These results suggest that endodermal expression of UGT76B1 is critical, as its absence in this specific root cell layer replicates the full-knockout phenotype.

UGT76B1 and FMO1 distinctly and specifically react to different types of soil microorganisms

To understand the biological significance of the constitutive expression of UGT76B1 and FMO1 in roots, we examined their responses to various soil-borne microorganisms. Microorganism-inoculated roots of *UGT76B1_{pro}::mTFP-UGT76B1* and *FMO1_{pro}::FMO1-YFP* plants were examined via confocal microscopy. In mock-treated plants, mTFP-UGT76B1 was present in the cortex and endodermis, whereas FMO1-YFP was barely detectable without enhanced camera sensitivity (Fig. 4a). Upon interaction with endophytic fungi, including three *Trichoderma* species and *Serendipita indica*, mTFP-UGT76B1 signals disappeared following root colonization by hyphae, whereas FMO1-YFP was induced in the pericycle with varying intensities (Fig. 4a,b). Similarly, inoculation with (hemi)biotrophic fungi including three *Fusarium* species, *Phytophthora parasitica* and *Sclerotinia sclerotiorum* led to enhanced FMO1-YFP paralleled by decreased mTFP-UGT76B1 expression. In contrast, necrotrophic pathogens such as *Botrytis cinerea* and two *Alternaria* species caused UGT76B1 suppression without FMO1 induction. This pattern was also observed upon inoculation with three

non-host pathogens, including the tree pathogens *Heterobasidion annosum* and *Verticillium albo-atrum* and the wheat pathogen *Ustilago nuda*. Additionally, inoculation with non-host mycorrhizae *Laccaria bicolor*, *Purpureocillium lilacinum* and *Meliniomyces bicolor* had no obvious effect (Fig. 4a). To confirm the spatial expression of FMO1, an *F. culmorum*-infected root was analysed showing that FMO1-YFP induction was restricted to the pericycle (Fig. 4b).

Since both endophytes and (hemi)biotrophs lead to similar responses, we selected two pairs of functionally divergent fungi from representative genera and species. Upon inoculation, we examined both the local sites of hyphae-colonized roots and distal, still-uninfected parts of the roots. The *Arabidopsis* beneficial root endophyte *Colletotrichum tofieldiae* (Ct) altered UGT76B1 and FMO1 expression only locally, whereas its pathogenic relative, *C. incanum* (Ci), led to the loss of mTFP-UGT76B1 and induction of FMO1 even in the distal parts of the root. A similar situation was observed with the beneficial *F. oxysporum* strain *Fo47* and the pathogenic strain *Fo5176* (Fig. 4c).

To investigate the dynamics of UGT76B1 and FMO1 regulation, root samples were monitored at multiple time points after inoculation with the fast-growing endophyte *Trichoderma harzianum*. mTFP-UGT76B1 rapidly disappeared, becoming undetectable within three hours, while FMO1-YFP induction appeared only after 18 h (Extended Data Fig. 5). To further explore this switch, we examined roots two and four days after *Ci* inoculation. The initial induction of FMO1-YFP in the pericycle disappeared in severely infected roots. mTFP-UGT76B1 expression did not recover in the cortex and endodermis but was instead induced in the stele (Extended Data Fig. 6). This regulation of the proteins in roots was also reflected at the transcript and metabolite levels in roots and shoots. *UGT76B1* transcripts were downregulated in roots after *Ci* inoculation, while both genes were upregulated in shoots. Expression data from several root-microbe/plant interactions corroborate the modulation of *UGT76B1* and *FMO1* (Supplementary Table 1). Consistently, NHP levels were significantly higher in roots and shoots of inoculated plants, whereas NHP-*O*-Gluc accumulated in shoots and decreased in roots (Extended Data Fig. 7a,b).

To determine whether the rapid loss of mTFP-UGT76B1 upon microbial interaction resulted from accelerated degradation or repressed translation of a high-turnover protein, we inhibited protein synthesis using cycloheximide. Under these conditions, mTFP-UGT76B1 remained stable for at least three days. Furthermore, a constitutively expressed mTFP-UGT76B1 disappeared one day after *Trichoderma* inoculation (Extended Data Fig. 8a,b). Thus, the rapid response to microorganisms is probably due to actively initiated degradation. Overall, both FMO1 and UGT76B1 are specifically and frequently oppositely regulated during interactions with different soil microorganisms.

Dosage effect of NHP on plant growth and defence

Both endophytes and (hemi)biotrophs probably manipulate root NHP levels by modulating FMO1 and UGT76B1 expression. In addition to impacts on defence, endophytes used in this study have been shown to promote plant growth. High endogenous NHP leads to retarded growth^{32–34,45}, also by downregulation of growth-related genes²⁶, while exogenous NHP feeding has a dosage-dependent effect on shoot defence level³⁹.

We therefore hypothesized that microorganism-modulated root NHP may have a dosage-dependent effect on plant growth and defence. To test this, we supplied different concentrations of NHP to soil-grown plants. We observed that low concentrations of NHP promoted plant growth, whereas high concentrations suppressed it (Fig. 5a and Extended Data Fig. 9a). A similar trend was observed when plants were grown on NHP-supplemented agar plates (Extended Data Fig. 9b).

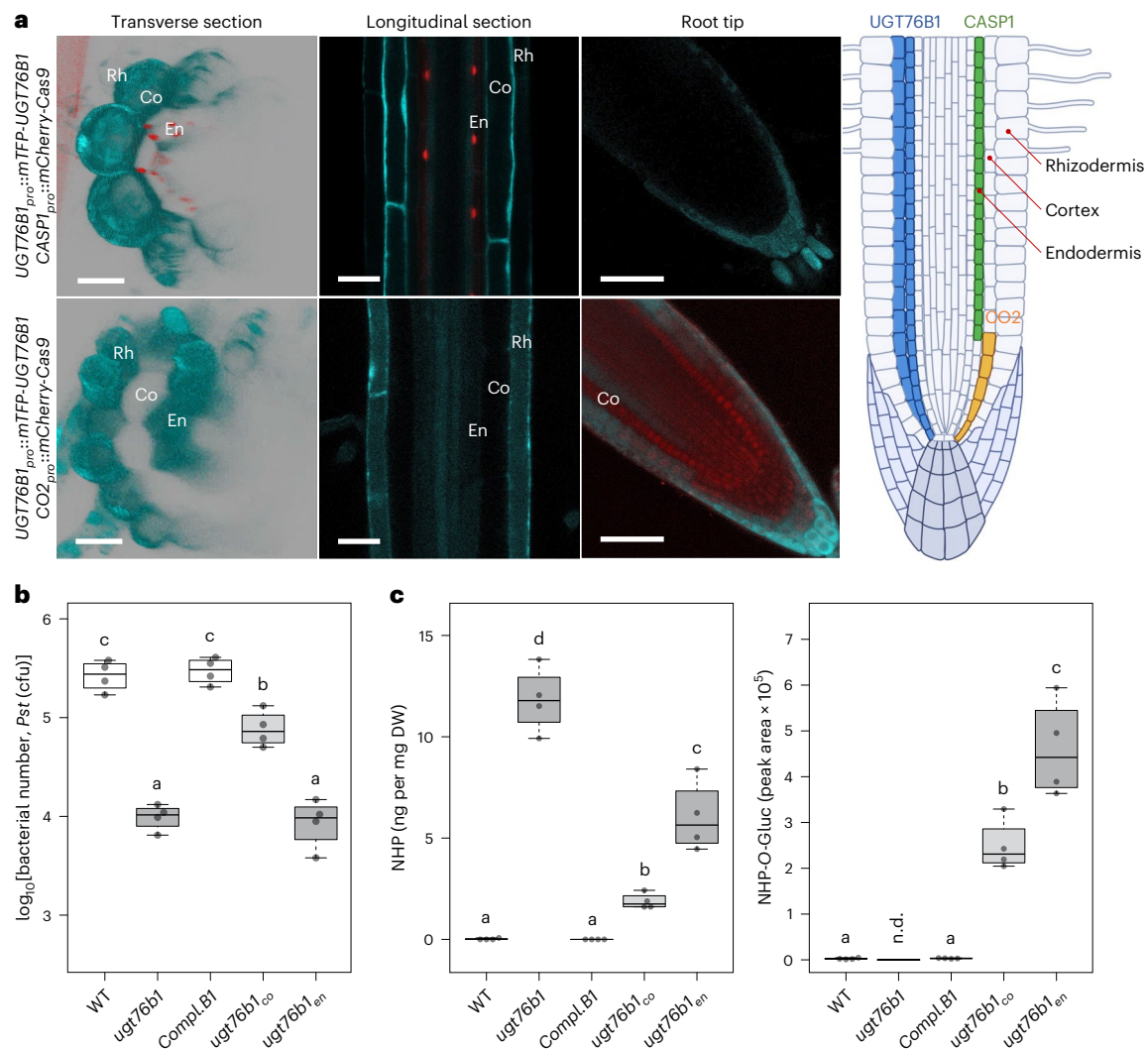


Fig. 3 | Differential impact of TSKO of UGT76B1 in root cell layers on shoot defence response. a, Confocal microscopy visualization of TSKO in 12-day-old plants grown on half-strength MS medium. The mTFP-UGT76B1 signal is shown in cyan, while mCherry-Cas9 driven by the *CASP1* and *CO2* promoters is detected in cortex initial and endodermal cells, respectively. The mTFP-UGT76B1 signal is abolished in tissues where mCherry-Cas9 is expressed from the *CASP1_{pro}::mCherry-Cas9* and *CO2_{pro}::mCherry-Cas9* constructs. *CO2_{pro}::mCherry-Cas9* is expressed in cortex initial cells, efficiently knocking out the gene and resulting in the absence of the mTFP-UGT76B1 signal in differentiated cortex cells. Transverse sections were obtained via optical cross section from longitudinal Z-stacks. Scale bars, 30 μ m. The experiment was repeated three times with similar results. **b**, Infection of four-week-old TSKO

lines with *Pst* DC3000. The absence of UGT76B1 in the endodermis replicates the defence response observed in whole-plant knockouts, whereas its removal from the cortex layer results in moderately enhanced defence against the pathogen. The experiments were repeated four times. **c**, NHP and NHP-O-Gluc levels in the shoots of TSKO lines. *ugt76b1_{en}* and, to a lower extent, *ugt76b1_{co}* leaves contain enhanced NHP and NHP-O-Gluc levels compared with the WT. These measurements were performed once with $n = 4$ independent samples. The boxes (**b**, **c**) represent the IQR (Q1–Q3), with the median shown as a bold line. The whiskers extend to $1.5 \times$ IQR. Significant differences between genotypes were analysed using one-way ANOVA with post hoc Tukey's test, as indicated by the letters ($P_{\text{adj}} < 0.05$). Root section graphic in **a** created with BioRender.com.

To determine whether some endophyte-induced growth promotion depends on NHP, we inoculated WT, *fmo1*, *ugt76b1* and NahG *sid2* with the plant growth-promoting fungus *T. harzianum* and monitored their growth. After 18 days, WT plants exhibited a significantly larger rosette area than mock-treated controls, while no growth promotion was observed for *fmo1* and *ugt76b1* mutants. NahG *sid2* plants showed suppressed growth upon *T. harzianum* inoculation (Extended Data Fig. 10).

To confirm that NHP mediated the root-microorganism-triggered shoot defence, we inoculated the roots of WT and *fmo1* plants with *Ct*, *Ci*, *Fo47* or *Fo5176*. Rosettes were harvested for metabolic analysis three days post-inoculation. NHP was found in WT shoots inoculated with fungi but undetectable in mock-treated and *fmo1* plants (Fig. 5b). Similarly, endogenous SA levels were elevated only in fungus-inoculated

WT plants (Fig. 5c). Plants were also infected by *Pst* four days after fungal inoculation. The WT exhibited enhanced resistance, which was abolished in *fmo1* (Fig. 5d).

To evaluate the early response to root-associated microorganisms, one-week-old seedlings were inoculated with conidia from four different fungi, and their growth was monitored. One week post inoculation, prior to the pathogens entering the necrotrophic phase and causing visible disease symptoms, WT plants inoculated with the pathogen *Fo5176* exhibited a significant reduction in growth. Inoculation with *Ci* also led to a numerically lower rosette area, whereas endophytic fungi *Ct* and *Fo47* did not alter growth. This phenomenon was also abolished in *fmo1* plants (Fig. 5e). In summary, certain root endophytes trigger shoot immunity and promote growth via NHP, whereas (hemi)biotrophs may lead to higher NHP levels, stronger immunity and retarded growth.

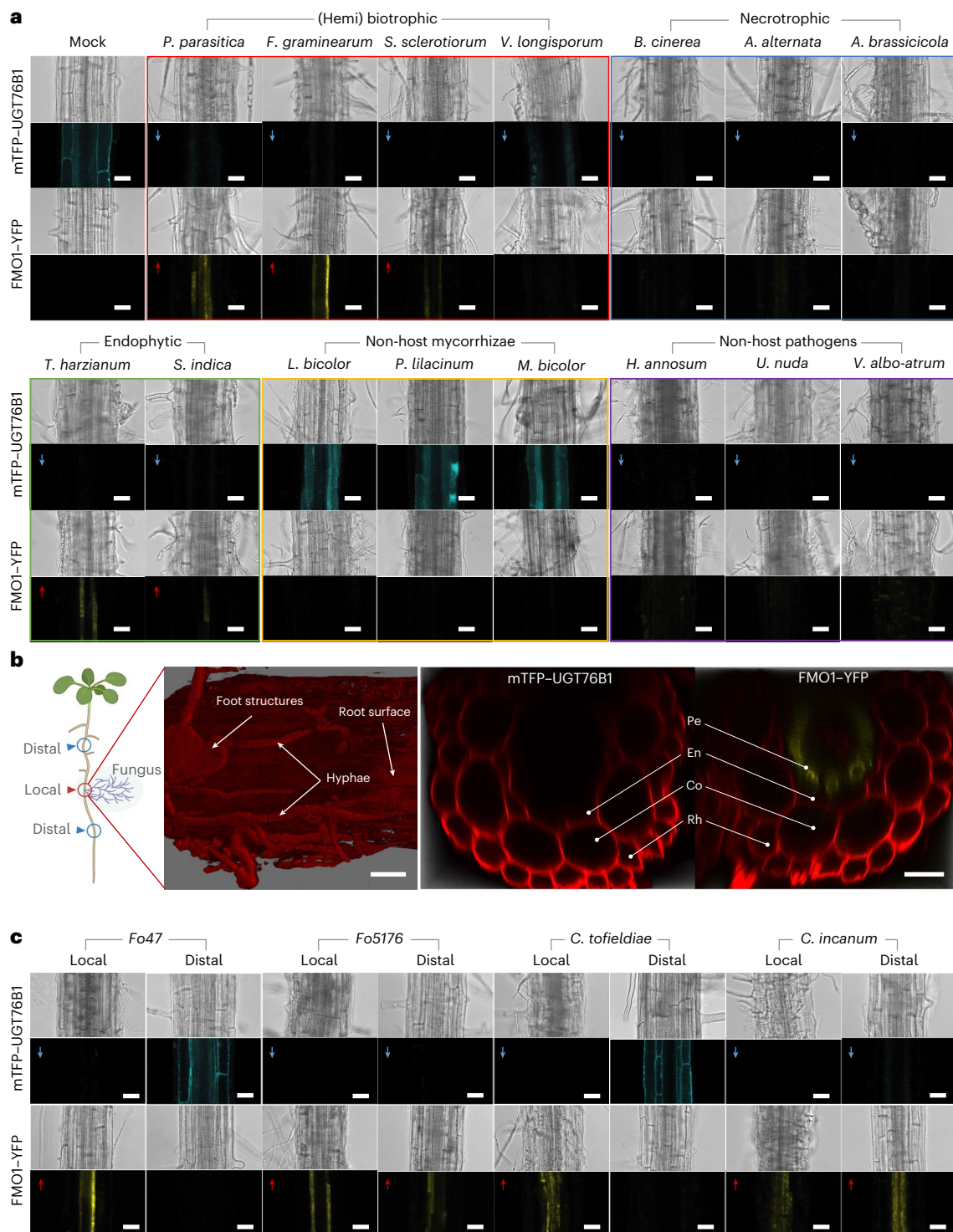


Fig. 4 | Differential responses of UGT76B1 and FMO1 expression in roots to fungal interactions. a, The expression of fluorescently labelled UGT76B1 and FMO1 proteins in response to inoculation with different types of fungi was monitored via confocal microscopy. Two-week-old plants grown on half-strength MS plates were inoculated with fungal plugs next to the root. One or two days after inoculation, roots colonized with fungal mycelium were examined. Blue arrows indicate downregulation of UGT76B1 compared with mock conditions; red arrows indicate upregulation of FMO1. *S. sclerotiorum*, previously classified as a necrotroph, has an early biotrophic phase explaining the observed

regulation. Scale bars, 30 μ m. **b**, Surface view and cross section of a root infected with *F. culmorum*. Fungal hyphae and root cells are visualized via propidium iodide staining. The expression of UGT76B1 in the cortex and endodermis is absent, while FMO1 is strongly induced in pericycle cells. Pe, pericycle. Scale bars, 20 μ m. **c**, UGT76B1 and FMO1 signal in local and distal root areas inoculated with beneficial or pathogenic fungi examined via confocal microscopy; distal regions are taken from uninfected root areas examined about 1 cm up/downstream of the fungal inoculation. Fo47, *Fusarium oxysporum* 47; Fo5176, *Fusarium oxysporum* 5176. Scale bars, 30 μ m. All experiments were repeated twice with similar results.

Discussion

Roots are vital for land plants to provide physical support and to acquire nutrients and water. Roots also exchange information with shoot tissue in a reciprocal manner. Among these interactions, induced systemic resistance *sensu stricto* is a well-studied mechanism on how root-interacting microorganisms establish JA- and ET-dependent and *PR*-gene-independent resistance against pathogens and herbivores in shoots^{1,46}. However, other instances, even among the same microbial genus, do not follow these hallmarks, and root-induced shoot resistance depends on SA^{14,47} (Supplementary Table 1). Yet, in both cases, the original trigger emanating from roots remains largely unknown. Here we show that numerous root-interacting fungi exploit components of the leaf-to-leaf SAR, but in a different setting. While SAR is established in leaves by initiating FMO1 expression upon a primary infection to produce the NHP signal, which is later attenuated by the induction of the NHP-conjugating UGT76B1, FMO1 and UGT76B1 exhibit a high basal expression level in naïve *Arabidopsis* roots to synthesize NHP and to concurrently confine its mobility via glucosylation. Upon contact with specific soil microorganisms, this balance is rapidly shifted by the suppression of UGT76B1 and/or upregulation of FMO1. The leaf SAR mechanism of switch-on and keep-in-check is thus altered in case of this root-triggered systemic resistance (RSR) into a standby mode with parallelly active FMO1 and UGT76B1 (Fig. 6). Interestingly, both beneficial and pathogenic microorganisms use this FMO1/UGT76B1 module, albeit with varying intensity. In contrast, non-host mycorrhizae used in this study did not cause effects, probably due to their lack of interaction with *Arabidopsis* roots. We suggest that microbial stimuli at the root are thereby integrated to affect shoot growth and/or defence status via the same principal mechanism. This is supported by the dose-dependent action of NHP not only to activate defence³⁹ but also to induce rather than suppress growth at lower NHP levels (Figs. 5 and 6). In naïve plants, the suppression of the shoot defence status is dependent on root-expressed UGT76B1, since *ugt76b1*/WT grafts showed WT-like *PR* gene expression in shoots (Fig. 2a). Thus, the suppressed NHP release from the WT roots does not overcome a defence-activating threshold in leaves despite the absence of UGT76B1.

Beneficial endophytes such as *Fo47* and *Ct* interacting with mature roots usually do not enter the vasculature^{22,48} and lead to localized

regulation of FMO1 and UGT76B1 at the root–microbe interface, releasing low amounts of NHP to the shoot to promote growth and moderately enhance resistance. In contrast, some (hemi)biotrophic pathogens such as *Fo5176* and *Ci* can colonize the vasculature^{22,48}

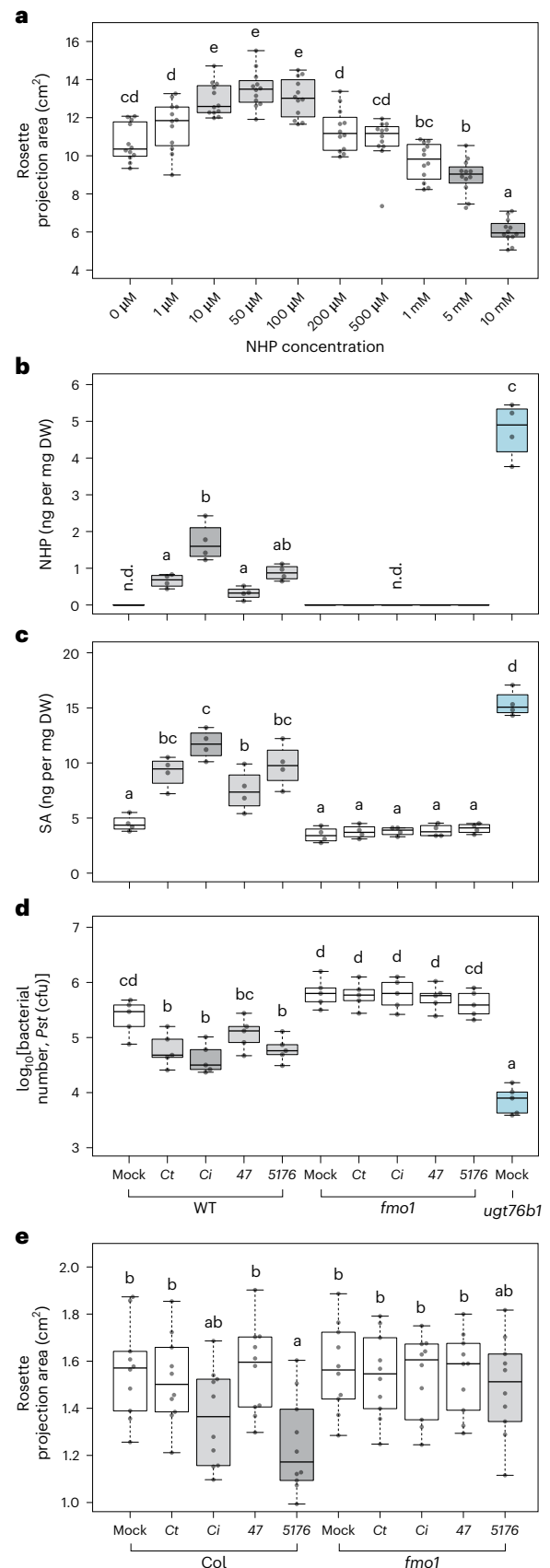


Fig. 5 | Fungal inoculation effects on growth and immunity mediated by NHP.

a, Plants were cultivated on soil supplemented with varying concentrations of NHP. The x axis represents different concentrations of NHP; 2 ml of NHP solution was supplied around the roots twice a week. Growth was assessed by recording the rosette projection area and fresh weight three weeks post-treatment (Extended Data Fig. 9). The results indicate that low concentrations of NHP stimulate plant growth, whereas high concentrations inhibit it. $n = 12$. Grey boxes indicate groups significantly different from the mock. **b–d**, Four-week-old WT and *fmo1* plants were root-inoculated with different fungi; *ugt76b1* (blue) was used as a reference. Shoots were harvested for analysis. WT plants inoculated with different root fungi showed enhanced leaf NHP levels, which were undetectable in mock-treated WT and *fmo1* plants (**b**). *ugt76b1* exhibited high levels of NHP. 47, *Fusarium oxysporum* 47; 5176, *Fusarium oxysporum* 5176. Root inoculation triggered leaf SA accumulation in the WT but not in *fmo1* (**c**). Four days after fungal inoculation, leaves of the WT and *fmo1* were challenged with *Pst* DC3000 (**d**). WT plants inoculated with *Ct*, *Ci* and 5176 exhibited stronger resistance than mock-treated WT plants, an effect abolished in *fmo1* plants. $n = 4$. **e**, One-week-old plants subjected to fungal inoculations displayed differential growth responses; the rosette projection area at day 7 post-inoculation is shown. The WT exhibited suppressed growth when inoculated with pathogenic fungi, whereas *fmo1* was unresponsive to fungal inoculation. $n = 10$. The experiments were repeated three times (**a**) or twice (**b–e**) with similar results. The boxes represent the IQR (Q1–Q3), with the median shown as a bold line. The whiskers extend to $1.5 \times$ IQR. Significant differences between genotypes and/or treatments were analysed using one-way (**a**) or two-way (**b–e**) ANOVA with post hoc Tukey's test (**a,d,e**) or the Lincon test (**b,c**), as indicated by the letters ($P_{adj} < 0.05$).

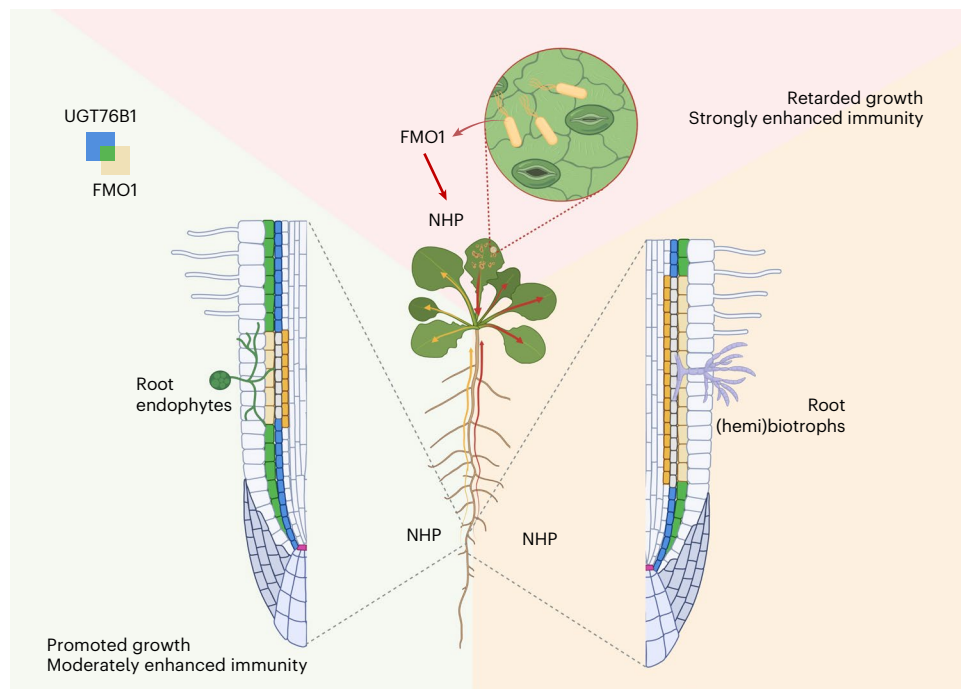


Fig. 6 | Root-triggered systemic resistance. FMO1 is not expressed in leaves of naïve plants. Upon pathogen attack, FMO1 is induced, and NHP is synthesized de novo. NHP can move systemically to enhance immunity also in distant leaves, a phenomenon known as SAR. In contrast, NHP is continuously synthesized and deactivated in roots due to the simultaneous presence of FMO1 and UGT76B1 establishing a signalling module on hold. Microorganisms differentially affect this 'inactive' NHP standby circuit. Endophytic fungi suppress UGT76B1 and promote FMO1 strictly at sites of root–fungus interaction. Biotrophic pathogens

elicit a similar response but across a more extended area around the site of interaction. These scenarios lead to different amounts of mobile NHP released from root to shoot; a low level of translocated NHP leads to promoted growth and moderately enhanced immunity, whereas higher levels of NHP provoke retarded growth and more strongly enhanced immunity. Exclusive and overlapping expression of UGT76B1 and FMO1 is shown by the indicated colour code. Figure created with [BioRender.com](https://www.biorender.com).

(Extended Data Fig. 6) and induce additional distal responses, potentially due to the spread of pathogen-associated molecular patterns or phytotoxins⁴² extending FMO1 and UGT76B1 regulation beyond the site of interaction. This probably leads to a stronger release of NHP, causing reduced growth and a significantly heightened SA-related resistance response in shoots (Figs. 5 and 6 and Extended Data Fig. 9). RSR thus shares key signalling components with SAR and provides a mechanistic explanation of previously identified SA-dependent systemic resistance triggered by root-associated microorganisms, such as *F. oxysporum*^{49,50} or *Trichoderma*⁵¹.

Despite the antagonistic relationship between JA/ET and SA signalling, induced systemic resistance *sensu stricto* and RSR elucidated here may also be interwoven, since some root endophytes have been reported to activate both pathways in shoots (for example, *T. virens* and *T. atroviride* or the endophyte *P. indica*)^{12,52}. Vice versa, different strains of one species, *P. simiae* (*fluorescens*), may activate JA/ET- or SA-dependent immunity^{14,46} (Supplementary Table 1). These findings may well align with our observations of UGT76B1 and FMO1 regulation—for example, still-active JA signalling in *fmo1* mutants may explain the trend to repress rosette growth and to enhance resistance to *P. syringae* upon interaction with *Fo5176*, since resistance against *Fo5176* depends on both SA and JA pathways⁵³ (Fig. 5d,e).

The proper function of this standby FMO1/UGT76B1 module confining the export of NHP from naïve roots depends on efficient glucosylation of the constitutively synthesized NHP. It was thus surprising that unconjugated NHP is detectable in roots, although at a comparatively low level^{26,33} (0.5 versus, for example, 10 ng per mg DW 24 h after *Pseudomonas* infection in leaves; Fig. 1). However, several observations suggest that the spatial distribution of NHP is crucial apart from its overall root level. First, FMO1 expression peaks in the cortex, whereas UGT76B1 is strongly expressed in the cortex and in the

endodermis—that is, forming a barrier to NHP's further release to the vasculature. Second, in line with this interpretation, cell-type-specific loss of UGT76B1 in the endodermis, but not in the cortex, fully mimics the shoot phenotype of the *ugt76b1* knockout. Third, FMO1 is induced in pericycle cells by many hemi(biotrophic) and endophytic fungi adjacent to the phloem rather than in its original expression sites (Fig. 4)—that is, NHP production would occur past the main UGT76B1 barrier.

The diverse approaches to root–microorganism-dependent regulation of shoot immunity and growth based on different hormone signalling pathways^{54,55} may reflect microbial diversity and different environmental contexts. The rhizosphere harbours a greater diversity and density of microorganisms than the phyllosphere⁵⁶. Locally, this challenge primarily requires plants to distinguish between beneficial and harmful microorganisms. Soil moisture favours the activity and proliferation of soil microorganisms, enhancing the potential chances and risks at the root interface⁵⁷. Concurrently, moist soils are frequently coupled to higher air humidity and thereby enhanced microbial impact on the shoot organs⁵⁸. Some pathogens may also use the root entry route to colonize aerial parts⁵⁹. A rapid mechanism of root–shoot communication as provided by the root-based standby FMO1/UGT76B1 module of RSR may thus confer an adaptive advantage in a systemic context. Moreover, the very same module in roots can fuel dose-dependent NHP signalling to coordinate the growth and defence status of shoots and is adaptive to different lifestyles, benefits and threats of the interacting microorganisms (Fig. 6).

Methods

Plant materials and growth conditions

This study used *Arabidopsis thaliana* accession Columbia (WT) along with mutant and transgenic lines: *ugt76b1-1* (SAIL_1171A11)³⁶, *fmo1-1* (SALK_026163)⁶⁰, the SA-depleted double mutant *NahG sid2* (ref. 36),

sid2 ugt76b1, NahG *sid2 ugt76b1*, *fmo1 ugt76b1* (ref. 61), *UGT76B1_{pro}::GFP-GUS*³⁶, *FMO1_{pro}::GUS*⁴¹ and the *fmo1-1* complementing *FMO1_{pro}::FMO1-YFP*⁴². Plants were cultivated in a controlled growth chamber under a 10 h light/14 h dark cycle at 22/18 °C, 60/70% relative humidity and 120 $\mu\text{mol m}^{-2} \text{s}^{-1}$ light intensity (type 840 fluorescent lamps; Osram). They were grown on a mixture of peat-moss-based substrate (Floragard Multiplication substrate) and quartz sand (12:1). A proportion of 6:1 was used for plant growth and monitoring in the phenotyping facility (Photon Systems Instruments). For fungal inoculation assays, seeds were germinated on half-strength MS medium (Duchefa) supplemented with 0.5% sucrose, stratified at 4 °C for two days and subsequently grown under the same conditions described above.

PR gene expression analysis

RNA isolation, reverse transcription and quantitative PCR were performed according to Bauer et al.³³ to assess the transcript levels of *PR1*, *PR2* and *PR5* (Supplementary Table 3).

Fluorescent-protein-labelled *ugt76b1* complementation line

The transgenic line *UGT76B1_{pro}::mTFP-UGT76B1* was generated to complement the *ugt76b1-1* mutant by expressing an amino-terminal mTFP fusion of *UGT76B1* under the control of its native promoter. A Gibson assembly reaction (New England Biolabs) was used to fuse three fragments: (1) a 1,754-bp *UGT76B1* promoter region, (2) the mTFP coding sequence without a stop codon and (3) a *UGT76B1* gene segment including the ATG start codon and 505 bp of the 3' untranslated region (Supplementary Table 3). This construct was recombined via pDONR221 (Invitrogen; screen with 50 mg l⁻¹ kanamycin) into pAlligator2Δ35S (screen with 100 mg l⁻¹ spectinomycin), a modified version of pAlligator2 with the CaMV 35S promoter removed⁶². The deletion was achieved via restriction enzyme digestion with EcoRI and HindIII, followed by blunt-ending using T4 DNA ligase and religation. The final vector was used for *Agrobacterium*-mediated transformation of *ugt76b1-1* via the floral dip method⁶³. Segregation analysis identified two independent homozygous transgenic lines with single insertions.

TSKO

UGT76B1 cortex- and endodermis-specific knockout lines are based on the *UGT76B1_{pro}::mTFP-UGT76B1* complementation line. Plasmids for tissue-specific genome editing were generated via PCR amplification and GoldenGate cloning employing BsaI and BpiI (ThermoFisher)⁶⁴. Regulatory sequences of At2g36100 (*CASP1*) and At1g62500 (*Co2*) were amplified via PCR (Supplementary Table 3) and cloned into pAGM1251 (ref. 65) via BpiI restriction/ligation to yield pCK256 and pCK257. Subsequently, promoter elements were assembled with (NLS)mCherry-P2A (pCK237), zCas9i (pCK70) and rbcS-E9 (terminator, pJOG416) modules in pICH47742 to yield pCK259 and pCK260. These modules were further assembled in the Level 2 acceptor pJOG292 (ref. 66) together with a BsaI-excisable *ccdB* cassette, the FAST seed fluorescence marker⁶⁷ and either spraying 1:800 diluted commercial Basta for soil-grown plants (*CASP1*) or screening in half-strength MS medium containing 30 mg l⁻¹ hygromycin (*CO2*) resistance cassette to yield pDGE1075 and pDGE1076, respectively. To generate the final plant transformation vectors, sgRNA-coding oligonucleotides were cloned into the sgRNA shuttle vectors pDGE332 and pDGE334 (Supplementary Table 3), and the assembled sgRNA transcriptional units were mobilized into pDGE1075 or pDGE1076 to yield pDGE1075-B1en and pDGE1076-B1co. These binary vectors were transformed into *Agrobacterium tumefaciens* GV3101 pMP90 for plant transformation.

Histochemical analyses

For histochemical analyses of promoter–GUS reporter lines, plant tissues were stained⁶⁸ for 30 min (*UGT76B1_{pro}* plants) or 12 h (*FMO1_{pro}* plants). Chlorophyll was removed by destaining with 70% ethanol. Images were captured using a stereomicroscope (Zeiss Stemi 2000-C)

at ×20 magnification. Protein expression of *UGT76B1* and *FMO1* in roots was visualized using the *UGT76B1_{pro}::mTFP-UGT76B1* and *FMO1_{pro}::FMO1-YFP* lines, respectively, with a confocal laser scanning microscope (SP8, Leica). For cell wall staining, two-week-old seedlings grown on vertical agar plates were treated with 50 $\mu\text{g ml}^{-1}$ propidium iodide for 30 min and then rinsed twice with double-distilled water before imaging. An argon laser was used as the light source. mTFP was excited at 458 nm, with emission collected between 482 and 502 nm (laser intensity, 25%; 100% gain; pinhole set to 1). YFP was excited at 514 nm, with emission collected between 520 and 540 nm (laser intensity, 40%; 100% gain; pinhole set to 2.5). When co-detected with both fluorescent proteins, PI staining shared their excitation wavelengths and was detected between 626 and 646 nm. All confocal images were acquired with a ×40 water immersion objective lens, with an area size of 320 $\mu\text{m} \times 320 \mu\text{m}$ and a resolution of 1,024 × 1,024. In Fig. 4, the images were cropped to fit the layout; all other figures retain their original size.

Micrografting assay

The grafting protocol was adapted from a previous description⁶⁹. Seeds were sterilized and sown on half-strength MS medium without vitamins (Duchefa; 1% sucrose; 1% bacteriological agar, Roth). After two days of stratification, the plates were moved to a growth incubator (MLR 351H, Sanyo) and incubated for three days under constant light (50 $\mu\text{mol m}^{-2} \text{s}^{-1}$) at 22 °C; then the light intensity was reduced to 10 $\mu\text{mol m}^{-2} \text{s}^{-1}$ for two additional days to promote hypocotyl elongation. Seedlings were cut straight through the middle of the hypocotyls using a fresh razor blade, and rootstocks and scions were combined in the desired combinations on half-strength MS medium with 0.5% sucrose (see Supplementary Fig. 2 for a detailed operation illustration). The grafted seedlings were then grown vertically under constant light (10 $\mu\text{mol m}^{-2} \text{s}^{-1}$) at 27 °C for one week, followed by one week at 50 $\mu\text{mol m}^{-2} \text{s}^{-1}$ light under short-day conditions (10 h light at 22 °C; 14 h dark at 17 °C). Afterward, the plants were transferred to 120 × 120 mm square Petri dishes (Greiner Bio-One) containing 50 ml of half-strength MS medium without sucrose. Two weeks later, the plants were examined to exclude any fusions that had developed adventitious roots. Whole rosettes were harvested for gene expression analysis. For disease assays, the plants were moved to a slurry soil and grown covered with a lid for two days to maintain high humidity. They were then cultivated under regular conditions for another two weeks before the assay.

NHP feeding assay

For soil-grown plants, 2 ml of NHP solutions at concentrations of 1 μM , 10 μM , 50 μM , 100 μM , 200 μM , 500 μM , 1 mM, 5 mM and 10 mM were applied twice a week with a pipette to the soil around the roots of plants maintained under short-day conditions. Ten plants were used for each concentration. For plants grown on Petri dishes, seeds were sown on half-strength MS medium supplemented with NHP at concentrations of 0.2 μM , 1 μM , 5 μM , 10 μM , 50 μM , 100 μM and 250 μM (MedChem-Express). After two days of stratification, the plates were transferred to short-day conditions and positioned horizontally, with 16 plants for each concentration. Four-week-old soil-grown plants and 18-day-old plate-grown plants were imaged using an RGB camera, and the rosette area was measured using ImageJ for Mac (version 1.53K) software.

Microbial culture conditions and inoculation assay

The fungal and oomycete strains used in this study are listed in Supplementary Table 4. Strains were cultured at 22 °C on VJS agar medium⁷⁰ for *S. indica*, *V. longisporum* and *P. parasitica* or on PDA medium (Sigma-Aldrich) for all other strains. For conidia harvesting, corresponding strains were grown in VJS liquid medium or PD broth (Sigma-Aldrich) at 24 °C with shaking at 180 rpm. After four days of cultivation, the liquid cultures were filtered through cheesecloth to remove mycelium. The conidia suspension was then centrifuged at 2,000 g for 10 min at 4 °C, and the resulting pellet was washed twice

with 10 mM MES buffer (pH 5.8) and resuspended in 0.05% Tween 20 solution. Conidia were counted using a haemocytometer, and the suspension was adjusted to a final concentration of 10^6 conidia per ml. For plant inoculation, 5 ml of the prepared conidia suspension was applied to the soil around the roots of 12-day-old plants (for growth measurement) and four-week-old plants (for *Pst* disease assays), taking care to avoid direct contact between the conidia and the rosette.

Bacterial inoculation and infection assays

Fully developed leaves from four- to five-week-old plants were gently infiltrated with either 10 mM MgCl_2 (as a control) or suspensions of *Pst* DC3000 in 10 mM MgCl_2 . For basal resistance assays, plants inoculated with *Pst* ($\text{OD}_{600} = 0.0001$) were kept under standard growth conditions for three days. Leaf discs from three independent plants (three discs per plant, pooled to form one biological sample) were collected 2 and 72 h post-inoculation and immersed in 500 μl of 10 mM MgCl_2 containing 0.01% Silwet L77 (Momentum; via Obermeier). Bacterial growth was quantified as described previously⁷¹. Each treatment was replicated five times; the entire experiment was conducted independently twice. To assess root-induced resistance, four-week-old plants were inoculated with 5 ml of conidia suspension as described above, and three days later, the same leaf-based disease assay was performed.

LC–MS analyses

SA, NHP and NHP-*O*-Gluc were quantified using LC–MS following extraction from freeze-dried plant material³³. 5 μl of each extract was injected twice as technical replicates for the LC–MS analysis. NHP and NHP-*O*-Gluc were detected using positive ionization mode, while SA was measured in negative ionization mode. Authentic standards for SA (Sigma-Aldrich) and NHP (MedChemExpress) were used for identification and quantification.

Statistics

All experiments were repeated at least twice except for the data in Fig. 3c and Extended Data Fig. 9, which were added during revision. In all cases, a single experimental series was based on at least four independent biological samples. Statistical analyses were conducted using R version 4.4.1 for Mac (<https://www.r-project.org/>). For analysis, we employed the WRS2 package, which includes Wilcoxon's robust statistical methods. Robust one-way and two-way ANOVA were performed for multiple group comparisons using the *t1way* and *t2way* functions, respectively. Prior to selecting post hoc tests, we applied the Shapiro–Wilk and Levene's tests to assess the normality and homogeneity of variances, which determined the use of either the Lincon test or Tukey's honestly significant difference for post hoc comparisons. Welch's two-sample *t*-tests were used for pairwise comparisons between two groups. The types of statistics are indicated in the figure legends.

Reporting summary

Further information on research design is available in the Nature Portfolio Reporting Summary linked to this article.

Data availability

The original LC–MS and confocal microscopic data are available via OSF at <https://doi.org/10.17605/OSF.IO/HKX75> (ref. 72) and <https://doi.org/10.17605/OSF.IO/EV796> (ref. 73). Correspondence and requests for materials should be addressed to A.R.S. Source data are provided with this paper.

References

- Pieterse, C. M. J. et al. Induced systemic resistance by beneficial microbes. *Annu. Rev. Phytopathol.* **52**, 347–375 (2014).
- De Kesel, J. et al. The induced resistance lexicon: do's and don'ts. *Trends Plant Sci.* **26**, 685–691 (2021).
- Fu, Z. Q. & Dong, X. Systemic acquired resistance: turning local infection into global defense. *Annu. Rev. Plant Biol.* **64**, 839–863 (2013).
- Durrant, W. E. & Dong, X. Systemic acquired resistance. *Annu. Rev. Phytopathol.* **42**, 185–209 (2004).
- Conrath, U., Beckers, G. J. M., Langenbach, C. J. G. & Jaskiewicz, M. R. Priming for enhanced defense. *Annu. Rev. Phytopathol.* **53**, 97–119 (2015).
- Vlot, A. C., Klessig, D. F. & Park, S.-W. Systemic acquired resistance: the elusive signal(s). *Curr. Opin. Plant Biol.* **11**, 436–442 (2008).
- Vlot, A. C. et al. Systemic propagation of immunity in plants. *N. Phytol.* **229**, 1234–1250 (2021).
- Spoel, S. H. & Dong, X. Salicylic acid in plant immunity and beyond. *Plant Cell* **36**, 1451–1464 (2024).
- Conrath, U., Pieterse, C. M. J. & Mauch-Mani, B. Priming in plant–pathogen interactions. *Trends Plant Sci.* **7**, 210–216 (2002).
- Zeier, J. Metabolic regulation of systemic acquired resistance. *Curr. Opin. Plant Biol.* **62**, 102050 (2021).
- Pieterse, C. M. J. et al. *Pseudomonas simiae* WCS417: star track of a model beneficial rhizobacterium. *Plant Soil* **461**, 245–263 (2021).
- Contreras-Cornejo, H. A., Macías-Rodríguez, L., Beltrán-Peña, E., Herrera-Estrella, A. & López-Bucio, J. *Trichoderma*-induced plant immunity likely involves both hormonal- and camalexin-dependent mechanisms in *Arabidopsis thaliana* and confers resistance against necrotrophic fungi *Botrytis cinerea*. *Plant Signal. Behav.* **6**, 1554–1563 (2011).
- Salas-Marina, M. A. et al. Colonization of *Arabidopsis* roots by *Trichoderma atroviride* promotes growth and enhances systemic disease resistance through jasmonic acid/ethylene and salicylic acid pathways. *Eur. J. Plant Pathol.* **131**, 15–26 (2011).
- van de Mortel, J. E. et al. Metabolic and transcriptomic changes induced in *Arabidopsis* by the rhizobacterium *Pseudomonas fluorescens* SS101. *Plant Physiol.* **160**, 2173–2188 (2012).
- Tjamos, S. E., Flemetakis, E., Paplomatas, E. J. & Katinakis, P. Induction of resistance to *Verticillium dahliae* in *Arabidopsis thaliana* by the biocontrol agent K-165 and pathogenesis-related proteins gene expression. *Mol. Plant Microbe Interact.* **18**, 555–561 (2005).
- Martínez-Medina, A. et al. Deciphering the hormonal signalling network behind the systemic resistance induced by *Trichoderma harzianum* in tomato. *Front. Plant Sci.* **4**, 206 (2013).
- Mathys, J. et al. Genome-wide characterization of ISR induced in *Arabidopsis thaliana* by *Trichoderma hamatum* T382 against *Botrytis cinerea* infection. *Front. Plant Sci.* **3**, 108 (2012).
- Sommer, A. et al. A salicylic acid-associated plant–microbe interaction attracts beneficial *Flavobacterium* sp. to the *Arabidopsis thaliana* phyllosphere. *Physiol. Plant.* **176**, e14483 (2024).
- Weston, D. J. et al. *Pseudomonas fluorescens* induces strain-dependent and strain-independent host plant responses in defense networks, primary metabolism, photosynthesis, and fitness. *Mol. Plant Microbe Interact.* **25**, 765–778 (2012).
- Hacquard, S. et al. Survival trade-offs in plant roots during colonization by closely related beneficial and pathogenic fungi. *Nat. Commun.* **7**, 11362 (2016).
- Pérez-Alonso, M. et al. The calcium sensor CBL7 is required for *Serendipita indica*-induced growth stimulation in *Arabidopsis thaliana*, controlling defense against the endophyte and K^+ homeostasis in the symbiosis. *Plant Cell Environ.* **45**, 3367–3382 (2022).
- Martínez-Soto, D., Yu, H., Allen, K. S. & Ma, L.-J. Differential colonization of the plant vasculature between endophytic versus pathogenic *Fusarium oxysporum* strains. *Mol. Plant Microbe Interact.* **36**, 4–13 (2023).

23. Brotman, Y. et al. *Trichoderma*-plant root colonization: escaping early plant defense responses and activation of the antioxidant machinery for saline stress tolerance. *PLoS Path.* **9**, e1003221 (2013).
24. Bernsdorff, F. et al. Pipecolic acid orchestrates plant systemic acquired resistance and defense priming via salicylic acid-dependent and -independent pathways. *Plant Cell* **28**, 102–129 (2016).
25. Mishina, T. E. & Zeier, J. Pathogen-associated molecular pattern recognition rather than development of tissue necrosis contributes to bacterial induction of systemic acquired resistance in *Arabidopsis*. *Plant J.* **50**, 500–513 (2007).
26. Hartmann, M. et al. Flavin monooxygenase-generated *N*-hydroxypipecolic acid is a critical element of plant systemic immunity. *Cell* **173**, 456–469 (2018).
27. Maldonado, A. M., Doerner, P., Dixon, R. A., Lamb, C. J. & Cameron, R. K. A putative lipid transfer protein involved in systemic resistance signalling in *Arabidopsis*. *Nature* **419**, 399–403 (2002).
28. Jung, H. W., Tschaplinski, T. J., Wang, L., Glazebrook, J. & Greenberg, J. T. Priming in systemic plant immunity. *Science* **324**, 89–91 (2009).
29. Chanda, B. et al. Glycerol-3-phosphate is a critical mobile inducer of systemic immunity in plants. *Nat. Genet.* **43**, 421–427 (2011).
30. Wenig, M. et al. Systemic acquired resistance networks amplify airborne defense cues. *Nat. Commun.* **10**, 3813 (2019).
31. Park, S.-W., Kaimoyo, E., Kumar, D., Mosher, S. & Klessig, D. F. Methyl salicylate is a critical mobile signal for plant systemic acquired resistance. *Science* **318**, 113–116 (2007).
32. Cai, J. et al. Glycosylation of *N*-hydroxy-pipecolic acid equilibrates between systemic acquired resistance response and plant growth. *Mol. Plant* **14**, 440–455 (2021).
33. Bauer, S. et al. UGT76B1, a promiscuous hub of small molecule-based immune signaling, glucosylates *N*-hydroxypipecolic acid, and balances plant immunity. *Plant Cell* **33**, 714–734 (2021).
34. Mohnike, L. et al. The glucosyltransferase UGT76B1 modulates *N*-hydroxy-pipecolic acid homeostasis and plant immunity. *Plant Cell* **33**, 735–749 (2021).
35. Holmes, E. C., Chen, Y.-C., Mudgett, M. B. & Sattely, E. S. *Arabidopsis* UGT76B1 glucosylates *N*-hydroxy-pipecolic acid and inactivates systemic acquired resistance in tomato. *Plant Cell* **33**, 750–765 (2021).
36. von Saint Paul, V. et al. The *Arabidopsis* glucosyltransferase UGT76B1 conjugates isoleucic acid and modulates plant defense and senescence. *Plant Cell* **23**, 4124–4145 (2011).
37. Yildiz, I. et al. The mobile SAR signal *N*-hydroxypipecolic acid induces NPR1-dependent transcriptional reprogramming and immune priming. *Plant Physiol.* **186**, 1679–1705 (2021).
38. Löwe, M. et al. *N*-hydroxypipecolic acid primes plants for enhanced microbial pattern-induced responses. *Front. Plant Sci.* **14**, 1217771 (2023).
39. Schnake, A. et al. Inducible biosynthesis and immune function of the systemic acquired resistance inducer *N*-hydroxypipecolic acid in monocotyledonous and dicotyledonous plants. *J. Exp. Bot.* **71**, 6444–6459 (2020).
40. Noutoshi, Y. et al. Novel plant immune-priming compounds identified via high-throughput chemical screening target salicylic acid glucosyltransferases in *Arabidopsis*. *Plant Cell* **24**, 3795–3804 (2012).
41. Olszak, B. et al. A putative flavin-containing mono-oxygenase as a marker for certain defense and cell death pathways. *Plant Sci.* **170**, 614–623 (2006).
42. Joglekar, S. et al. Chemical activation of EDS1/PAD4 signaling leading to pathogen resistance in *Arabidopsis*. *Plant Cell Physiol.* **59**, 1592–1607 (2018).
43. Ryu, K. H., Huang, L., Kang, H. M. & Schiefelbein, J. Single-cell RNA sequencing resolves molecular relationships among individual plant cells. *Plant Physiol.* **179**, 1444–1456 (2019).
44. Fucile, G. et al. ePlant and the 3D data display initiative: integrative systems biology on the world wide web. *PLoS ONE* **6**, e15237 (2011).
45. Shields, A., Shrivnauth, V. & Castroverde, C. D. M. Salicylic acid and *N*-hydroxypipecolic acid at the fulcrum of the plant immunity–growth equilibrium. *Front. Plant Sci.* **13**, 841688 (2022).
46. Pieterse, C. M., Van Wees, S. C., Hoffland, E., Van Pelt, J. A. & Van Loon, L. C. Systemic resistance in *Arabidopsis* induced by biocontrol bacteria is independent of salicylic acid accumulation and pathogenesis-related gene expression. *Plant Cell* **8**, 1225–1237 (1996).
47. Pieterse, C. M. J. et al. A novel signaling pathway controlling induced systemic resistance in *Arabidopsis*. *Plant Cell* **10**, 1571–1580 (1998).
48. Hiruma, K. et al. Root endophyte *Colletotrichum tofieldiae* confers plant fitness benefits that are phosphate status dependent. *Cell* **165**, 464–474 (2016).
49. Lyons, R. et al. *Fusarium oxysporum* triggers tissue-specific transcriptional reprogramming in *Arabidopsis thaliana*. *PLoS ONE* **10**, e0121902 (2015).
50. Edgar, C. I. et al. Salicylic acid mediates resistance to the vascular wilt pathogen *Fusarium oxysporum* in the model host *Arabidopsis thaliana*. *Australas. Plant Pathol.* **35**, 581–591 (2006).
51. Alonso-Ramírez, A. et al. Salicylic acid prevents *Trichoderma harzianum* from entering the vascular system of roots. *Mol. Plant Pathol.* **15**, 823–831 (2014).
52. Pedrotti, L., Mueller, M. J. & Waller, F. *Piriformospora indica* root colonization triggers local and systemic root responses and inhibits secondary colonization of distal roots. *PLoS ONE* **8**, e69352 (2013).
53. Wang, L., Calabria, J., Chen, H.-W. & Somssich, M. The *Arabidopsis thaliana*–*Fusarium oxysporum* strain 5176 pathosystem: an overview. *J. Exp. Bot.* **73**, 6052–6067 (2022).
54. Pieterse, C. M. J., Van der Does, D., Zamioudis, C., Leon-Reyes, A. & Van Wees, S. C. M. Hormonal modulation of plant immunity. *Annu. Rev. Cell Dev. Biol.* **28**, 489–521 (2012).
55. Eichmann, R., Richards, L. & Schäfer, P. Hormones as go-betweens in plant microbiome assembly. *Plant J.* **105**, 518–541 (2021).
56. Trivedi, P., Leach, J. E., Tringe, S. G., Sa, T. & Singh, B. K. Plant–microbiome interactions: from community assembly to plant health. *Nat. Rev. Microbiol.* **18**, 607–621 (2020).
57. Schimel, J., Balser, T. C. & Wallenstein, M. Microbial stress-response physiology and its implications for ecosystem function. *Ecology* **88**, 1386–1394 (2007).
58. Chaudhry, V. et al. Shaping the leaf microbiota: plant–microbe–microbe interactions. *J. Exp. Bot.* **72**, 36–56 (2021).
59. Chuberre, C. et al. Plant immunity is compartmentalized and specialized in roots. *Front. Plant Sci.* **9**, 1692 (2018).
60. Mishina, T. E. & Zeier, J. The *Arabidopsis* flavin-dependent monooxygenase FMO1 is an essential component of biologically induced systemic acquired resistance. *Plant Physiol.* **141**, 1666–1675 (2006).
61. Zhang, W., Maksym, R., Georgii, E., Geist, B. & Schäffner, A. R. SA and NHP glucosyltransferase UGT76B1 affects plant defense in both SID2- and NPR1-dependent and independent manner. *Plant Cell Rep.* **43**, 149 (2024).
62. Bensmihen, S. et al. Analysis of an activated ABI5 allele using a new selection method for transgenic *Arabidopsis* seeds. *FEBS Lett.* **561**, 127–131 (2004).
63. Clough, S. J. & Bent, A. F. Floral dip: a simplified method for *Agrobacterium*-mediated transformation of *Arabidopsis thaliana*. *Plant J.* **16**, 735–743 (1998).

64. Stuttmann, J. et al. Highly efficient multiplex editing: one-shot generation of 8× *Nicotiana benthamiana* and 12× *Arabidopsis* mutants. *Plant J.* **106**, 8–22 (2021).
65. Engler, C. et al. A Golden Gate modular cloning toolbox for plants. *ACS Synth. Biol.* **3**, 839–843 (2014).
66. Ordon, J. et al. Generation of chromosomal deletions in dicotyledonous plants employing a user-friendly genome editing toolkit. *Plant J.* **89**, 155–168 (2017).
67. Shimada, T. L., Shimada, T. & Hara-Nishimura, I. A rapid and non-destructive screenable marker, FAST, for identifying transformed seeds of *Arabidopsis thaliana*. *Plant J.* **61**, 519–528 (2010).
68. Lagarde, D. et al. Tissue-specific expression of *Arabidopsis AKT1* gene is consistent with a role in K⁺ nutrition. *Plant J.* **9**, 195–203 (1996).
69. Christmann, A., Weiler, E. W., Steudle, E. & Grill, E. A hydraulic signal in root-to-shoot signalling of water shortage. *Plant J.* **52**, 167–174 (2007).
70. Osman, M., Stigloher, C., Mueller, M. J. & Waller, F. An improved growth medium for enhanced inoculum production of the plant growth-promoting fungus *Serendipita indica*. *Plant Meth.* **16**, 39 (2020).
71. Katagiri, F., Thilmony, R. & He, S. Y. The *Arabidopsis thaliana*–*Pseudomonas syringae* interaction. *Arabidopsis Book* **1**, e0039 (2002).
72. Schäffner, A. R. & Xu, P. Original LC–MS and confocal data of the study ‘A root-based N-hydroxyphenylpyruvic acid standby circuit to direct immunity and growth of *Arabidopsis* shoots’ part 1. *OSF* <https://doi.org/10.17605/OSF.IO/HKX75> (2025).
73. Schäffner, A. R. & Xu, P. Original LC–MS and confocal data of the study ‘A root-based N-hydroxyphenylpyruvic acid standby circuit to direct immunity and growth of *Arabidopsis* shoots’ part 2. *OSF* <https://doi.org/10.17605/OSF.IO/EV796> (2025).

Acknowledgements

A. Attard, G. Bahnweg, J. P. Benz, W. Dröge-Laser, S. Hacquard, M. Schmoll, J.-P. Schnitzler and C. Steinberg provided microorganisms. We thank J. Parker for providing the *FMO1_{pro}::FMO1-YFP* line and J. Mundy for the *FMO1_{pro}::GUS* line. We thank B. Geist and C. Kretschmer (University of Halle) for technical assistance. P.X. thanks the China Scholarship Council for a fellowship supporting his doctoral thesis. Q. Tang, T. Zhu, P. B. S. Padmanaban, J. Durner, C. Vlot-Schuster and J. Zeier provided valuable advice.

Author contributions

P.X. and A.R.S. conceptualized the study on the basis of the original grafting experiments and findings of R.M. J.S. and A.R.S. designed

and constructed vectors for TSKO approaches. P.X., S.F. and B.L. performed the experiments. P.X. and A.R.S. wrote the manuscript with contributions from J.S.

Funding

Open access funding provided by Helmholtz Zentrum München - Deutsches Forschungszentrum für Gesundheit und Umwelt (GmbH).

Competing interests

The authors declare no competing interests.

Additional information

Extended data is available for this paper at <https://doi.org/10.1038/s41477-025-02053-2>.

Supplementary information The online version contains supplementary material available at <https://doi.org/10.1038/s41477-025-02053-2>.

Correspondence and requests for materials should be addressed to Anton R. Schäffner.

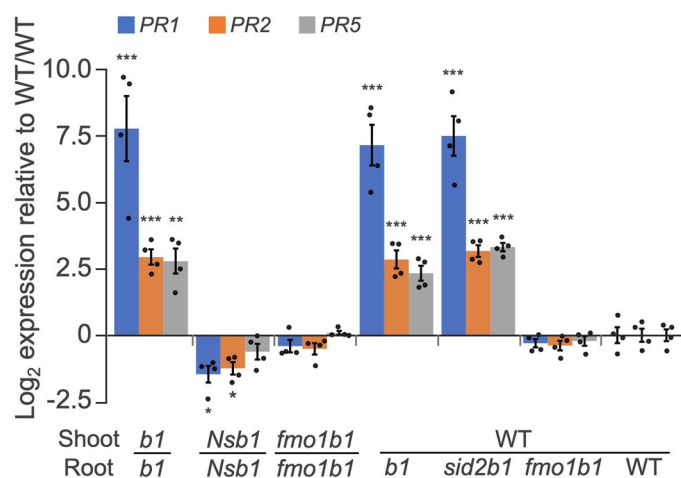
Peer review information *Nature Plants* thanks Asaph Aharoni, Jürgen Zeier and the other, anonymous, reviewer(s) for their contribution to the peer review of this work.

Reprints and permissions information is available at www.nature.com/reprints.

Publisher's note Springer Nature remains neutral with regard to jurisdictional claims in published maps and institutional affiliations.

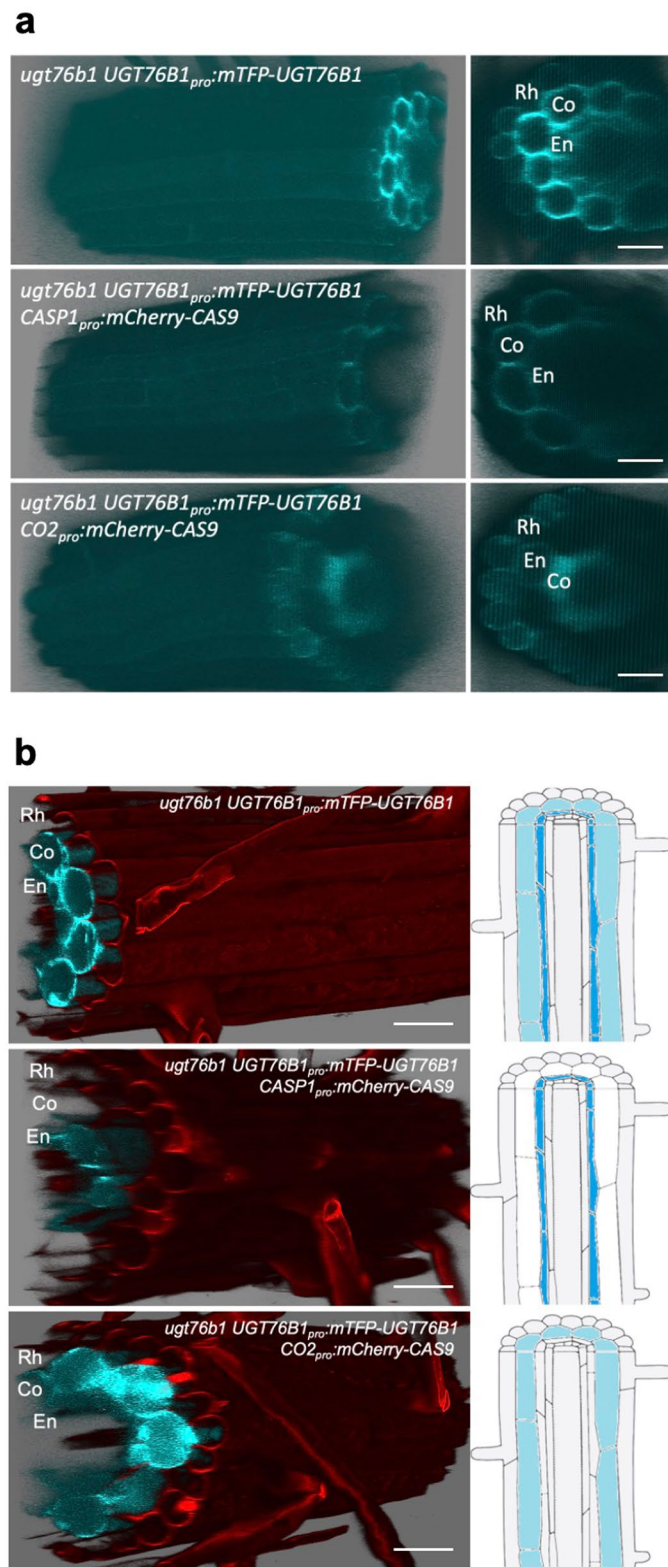
Open Access This article is licensed under a Creative Commons Attribution 4.0 International License, which permits use, sharing, adaptation, distribution and reproduction in any medium or format, as long as you give appropriate credit to the original author(s) and the source, provide a link to the Creative Commons licence, and indicate if changes were made. The images or other third party material in this article are included in the article's Creative Commons licence, unless indicated otherwise in a credit line to the material. If material is not included in the article's Creative Commons licence and your intended use is not permitted by statutory regulation or exceeds the permitted use, you will need to obtain permission directly from the copyright holder. To view a copy of this licence, visit <http://creativecommons.org/licenses/by/4.0/>.

© The Author(s) 2025



Extended Data Fig. 1 | *ugt76b1* root-mediated shoot resistance is dependent on root *FMO1*. Since NahG may hydroxylate other benzoic metabolites, the *sid2 ugt76b1* double mutant was also used in grafting experiments, showing a similar effect to that of NahG *sid2 ugt76b1*. Bars represent means \pm standard error of the

mean, $n = 4$. Significant differences between genotypes were analyzed using the Welch two-sample t-test (* $p < 0.05$, ** $p < 0.01$, *** $p < 0.001$). Experiments were independently repeated twice with similar results.

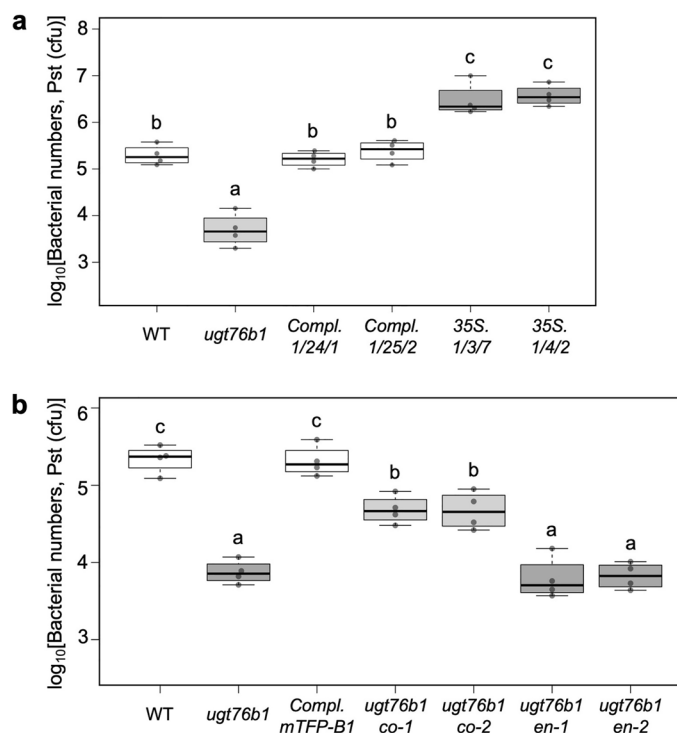


Extended Data Fig. 2 | See next page for caption.

Extended Data Fig. 2 | UGT76B1 expression in *ugt76b1* TSKO lines.

Twelve-day-old *UGT76B1pro::mTFP-UGT76B1* and *ugt76b1_{en}* and *ugt76b1_{co}* TSKO plants grown on half-strength MS medium and examined by confocal microscopy to visualize the cellular expression pattern of mTFP-UGT76B1 and the efficacy of the TSKO approach. **a**, Efficacy of TSKO approach. Plants were treated with 1 mM BTH by surface spraying to induce (mTFP-)UGT76B1 expression beyond its level in naïve roots. The main root was examined by confocal microscopy two days post-treatment. The mTFP-UGT76B1 signal (cyan) was enhanced at the same localization as in naïve plants (see **b** and Fig. 3a), specifically the cortex and endodermis, with weak induction in the epidermis. In the *ugt76b1_{en}* TSKO line,

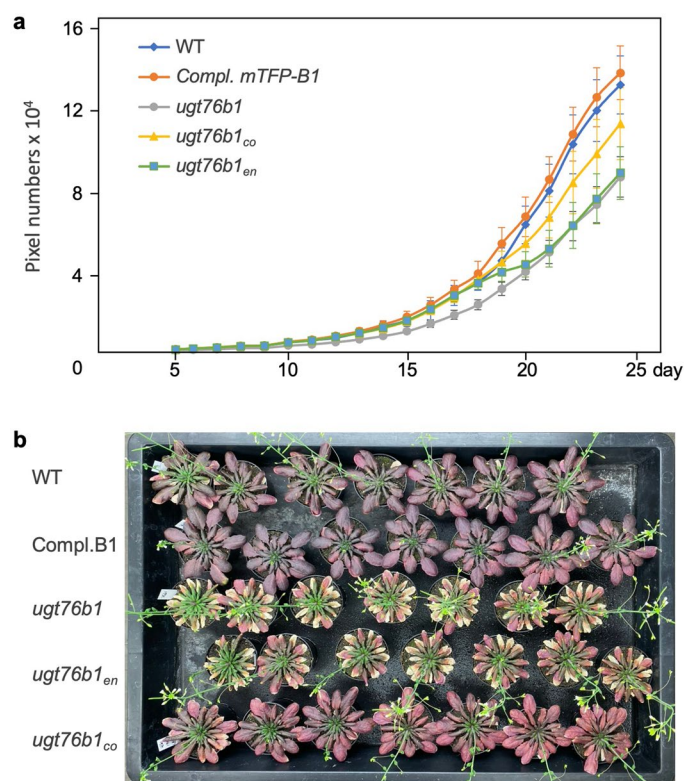
the endodermis signal is not visible even after BTH induction. In the *ugt76b1_{co}* TSKO line, the cortex signal is absent, although induction is still observed in the rhizodermis. Bar, 30 μ m. **b**, Illustration of three-dimensional UGT76B1 expression pattern in TSKO lines. Main roots of twelve-day-old plants grown on half-strength MS medium without BTH induction were used for confocal microscopy. mTFP-UGT76B1 is visualized in the cortex and endodermis. In the *ugt76b1_{co}* TSKO line, the mTFP signal is observed only in the endodermis. In the *ugt76b1_{en}* TSKO line, the endodermal signal is absent. En, endodermis; Co, cortex; Rh, rhizodermis. Bar, 30 μ m. The experiments were repeated three times (**a**) or twice (**b**) with similar results.



Extended Data Fig. 3 | Independent complementation and TSKO lines.

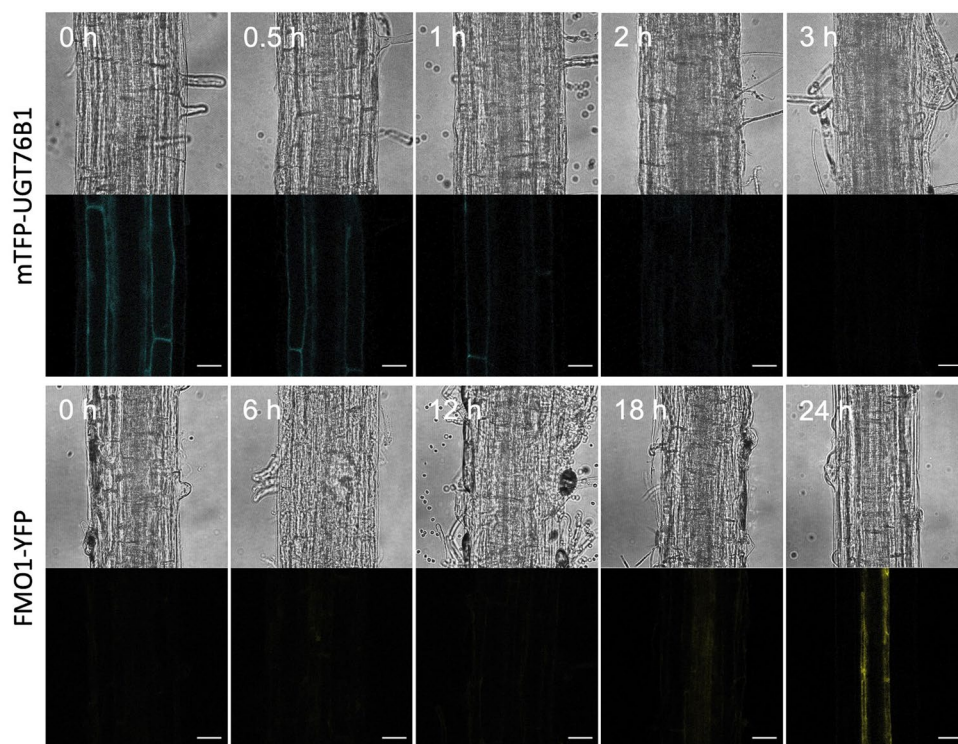
Sensitivity of independent complementation and TSKO lines towards infection with *Pst* DC3000. **a**, Two complementation lines (1/24/1 and 1/25/2), in which *ugt76b1* was complemented with the *UGT76B1_{pro}::mTFP-UGT76B1* construct. Line 1/25/2 was selected as the parental line for TSKO and used as a reference, named *Compl.mTFP-B1*. Additionally, two overexpression lines (1/3/7 and 1/4/2) carrying *35S_{pro}::mTFP-UGT76B1* were tested; line 1/4/2 was selected for further confocal microscopy analysis. **b**, The absence of UGT76B1 in the endodermis replicates the enhanced defense status observed in whole-plant knockouts, whereas its

removal from the cortex layer results in a moderately enhanced defense against the pathogen. Two independent cortex- and endodermis-specific knockout lines were obtained and tested for *Pst* proliferation. *ugt76b1co-1* and *ugt76b1en-2* were selected for repeated disease assays and microscopy analysis. The experiments (**a**, **b**) were independently repeated twice with similar results. Boxes represent the interquartile range (Q1–Q3), with the median shown as a bold line. Whiskers extend to $1.5 \times \text{IQR}$, $n = 4$. Significant differences between genotypes were analyzed using one-way ANOVA with post-hoc Tukey test, as indicated by letters ($p_{\text{adj}} < 0.05$).



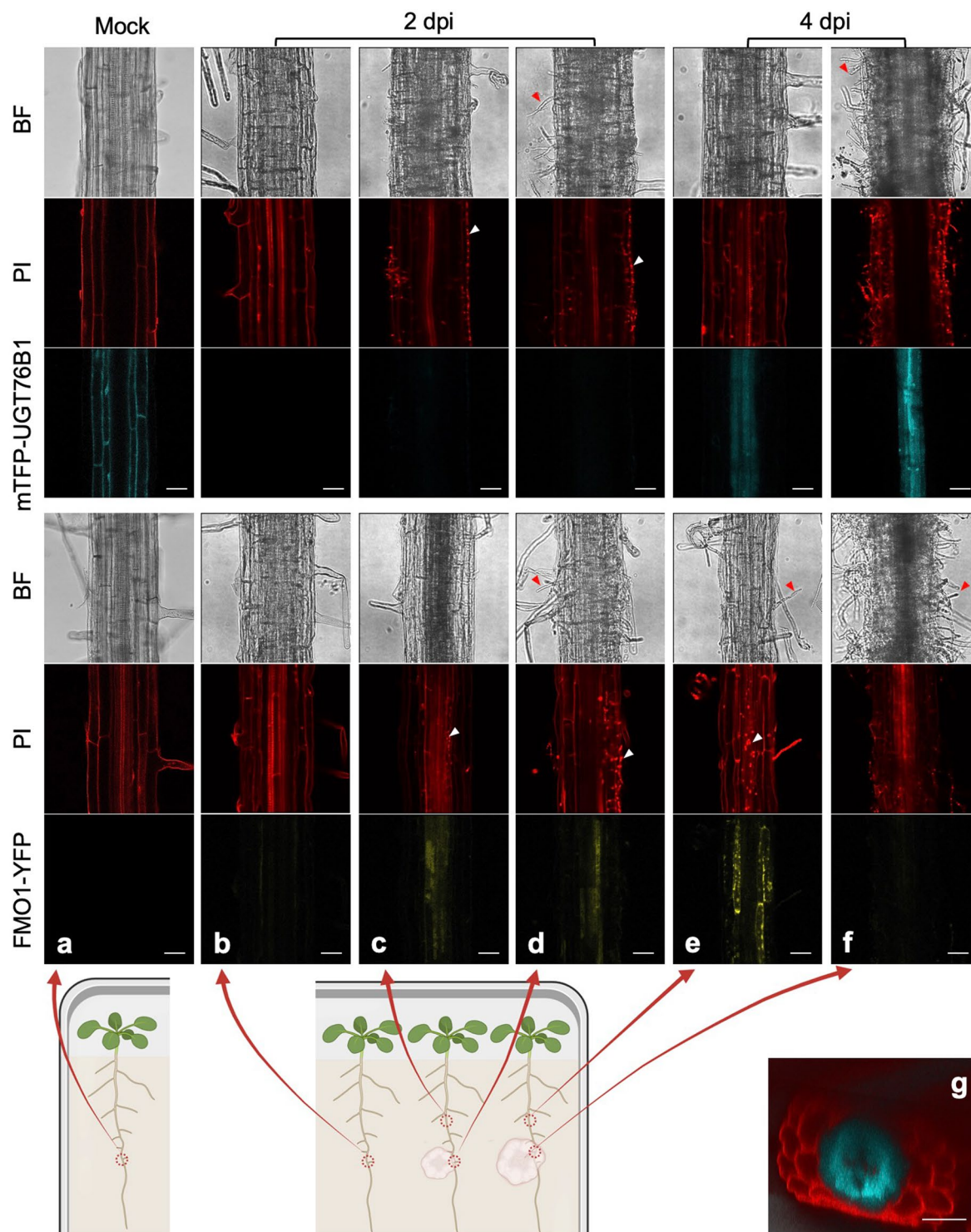
Extended Data Fig. 4 | Growth and leaf phenotypes. a, Growth monitoring of TSKO lines. Data collection began from 5-day-old plants; leaf projection area as a proxy for rosette growth was determined by the region with active chlorophyll fluorescence, measured daily at 6 a.m. (Extended Data Fig. 9a for a correlation of projected leaf area and fresh weight biomass). WT and the complementation line (*Compl.B1*) exhibit similar growth. *ugt76b1_{en}* shows a growth pattern similar to the *ugt76b1* mutant, whereas the growth of *ugt76b1_{co}* falls between that of WT and the *ugt76b1* mutant. $n = 12$, error bars represent standard deviation. **b**, Anthocyanin

accumulation and early senescence induced by day length shift. Four-week-old plants grown under short-day conditions were shifted to long-day conditions for an additional week. *ugt76b1* and *ugt76b1_{en}* exhibited similar early senescence, yellowing phenotypes, with less visible purple color in the leaves, indicating reduced anthocyanin accumulation. *ugt76b1_{co}* leaves displayed a visually lighter purple color compared to WT and the complementation line. Both experiments (**a**, **b**) were independently repeated twice with similar results.



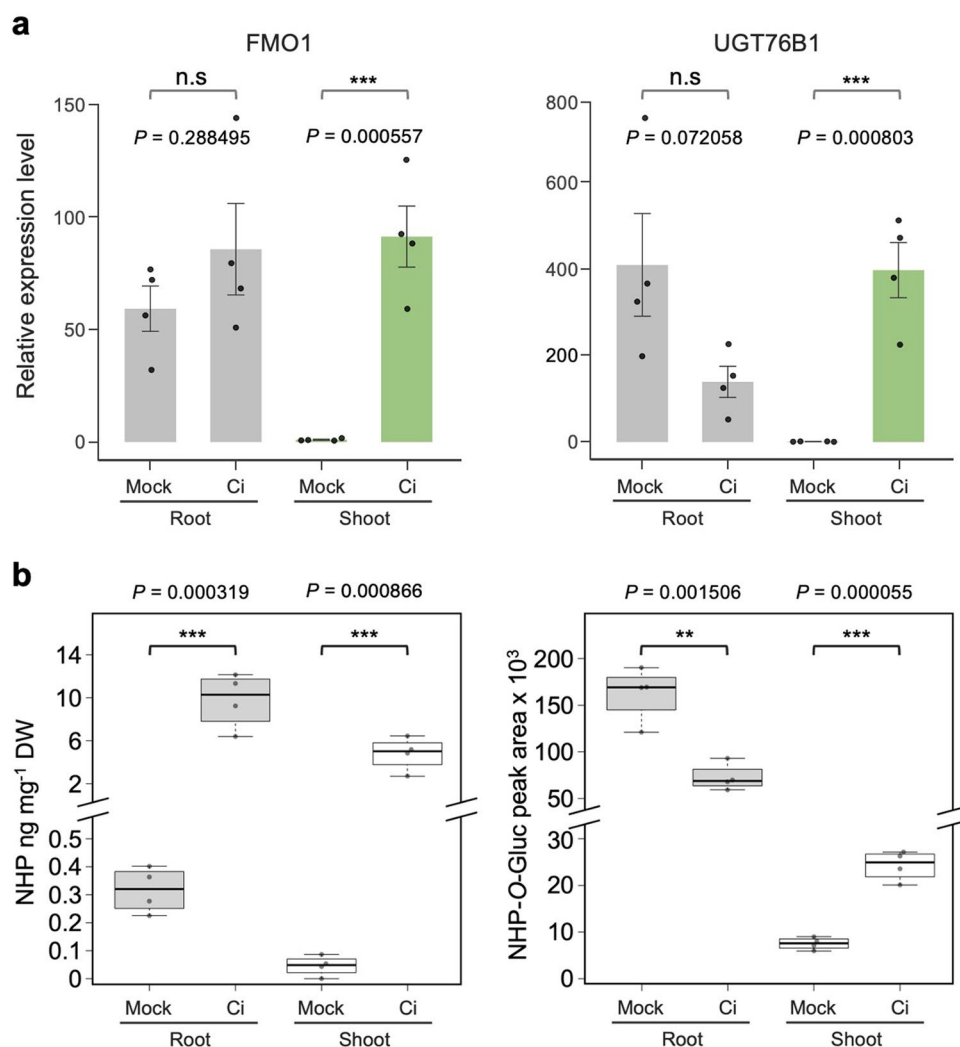
Extended Data Fig. 5 | Time course observation of UGT76B1 downregulation and FMO1 induction. Roots of mTFP-UGT76B1 and FMO1-YFP transgenic lines were observed in response to *T. harzianum*. An agar plug with mycelium was placed next to the root, allowing newly emerged hyphae to reach the root immediately. The mTFP-UGT76B1 signal began to fade within 1 h post-inoculation and was completely lost by 3 h. In contrast, FMO1-YFP was induced and became

visible after 18 h. Bar, 30 μm . An argon laser was used as the light source. mTFP was excited at 458 nm, with emission collected between 482 and 502 nm (laser intensity: 25%). YFP was excited at 514 nm, with emission collected between 520 and 540 nm (laser intensity: 40%). Imaging was performed using a 40 \times objective lens. The experiment was independently repeated twice with similar results.



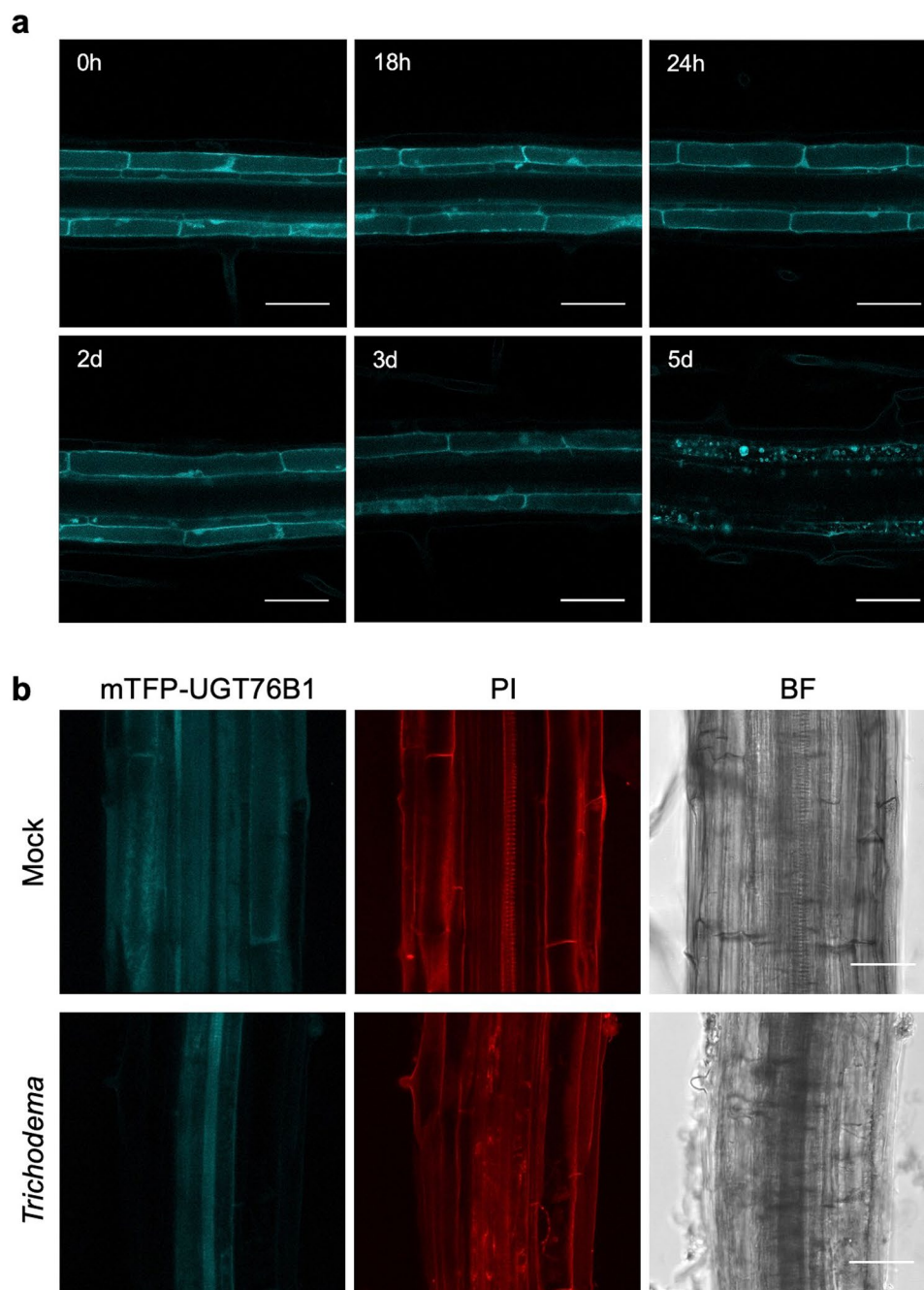
Extended Data Fig. 6 | Long-term infection with *C. incanum* (Ci). **a**, Mock-treated plants: mTFP-UGT76B1 is expressed in the cortex and endodermis, while FMO1-YFP is too weak to be detected at the chosen settings. **b**, Plants grown on plates inoculated with Ci for 2 days show complete loss of mTFP-UGT76B1 expression, even without direct contact to the fungus. **c-d**, Roots at distal and local sites of inoculation, 2 days post-inoculation (dpi). White arrows indicate fungal nuclei stained by propidium iodide. Ci penetrates the root, inducing FMO1

expression in the pericycle while keeping UGT76B1 expression suppressed. **e-f**, Roots at distal and local sites of inoculation, 4 dpi. **g**, mTFP-UGT76B1 expression in the stele. UGT76B1 is induced in the stele, while FMO1 expression in the pericycle disappears in severely infected roots and appears in the cortex and endodermis at regions distal to the inoculation site. BF, bright field; PI, propidium iodide staining. Bar, 30 μ m. The experiments were conducted once.



Extended Data Fig. 7 | Regulation of *UGT76B1*/*FMO1* expression and NHP metabolites upon *Ci* inoculation. Roots of 3-week-old *Arabidopsis* plants grown on half-strength MS plates were inoculated with *Ci* conidia. Each root was treated with 50 μ l of conidia solution containing 10^6 conidia/ml, evenly distributed on the root surface. Roots and shoots were harvested separately two days post-inoculation. To obtain sufficient root material, 25 plants were pooled per biological replicate. **a**, *UGT76B1* and *FMO1* expression levels were normalized to *Sl6* and *UBQ5*. Expression in roots only supports a tendency of upregulation of *FMO1* and downregulation of *UGT76B1*, respectively; however, these changes are in line with a local response leaving other parts of the harvested root unaffected.

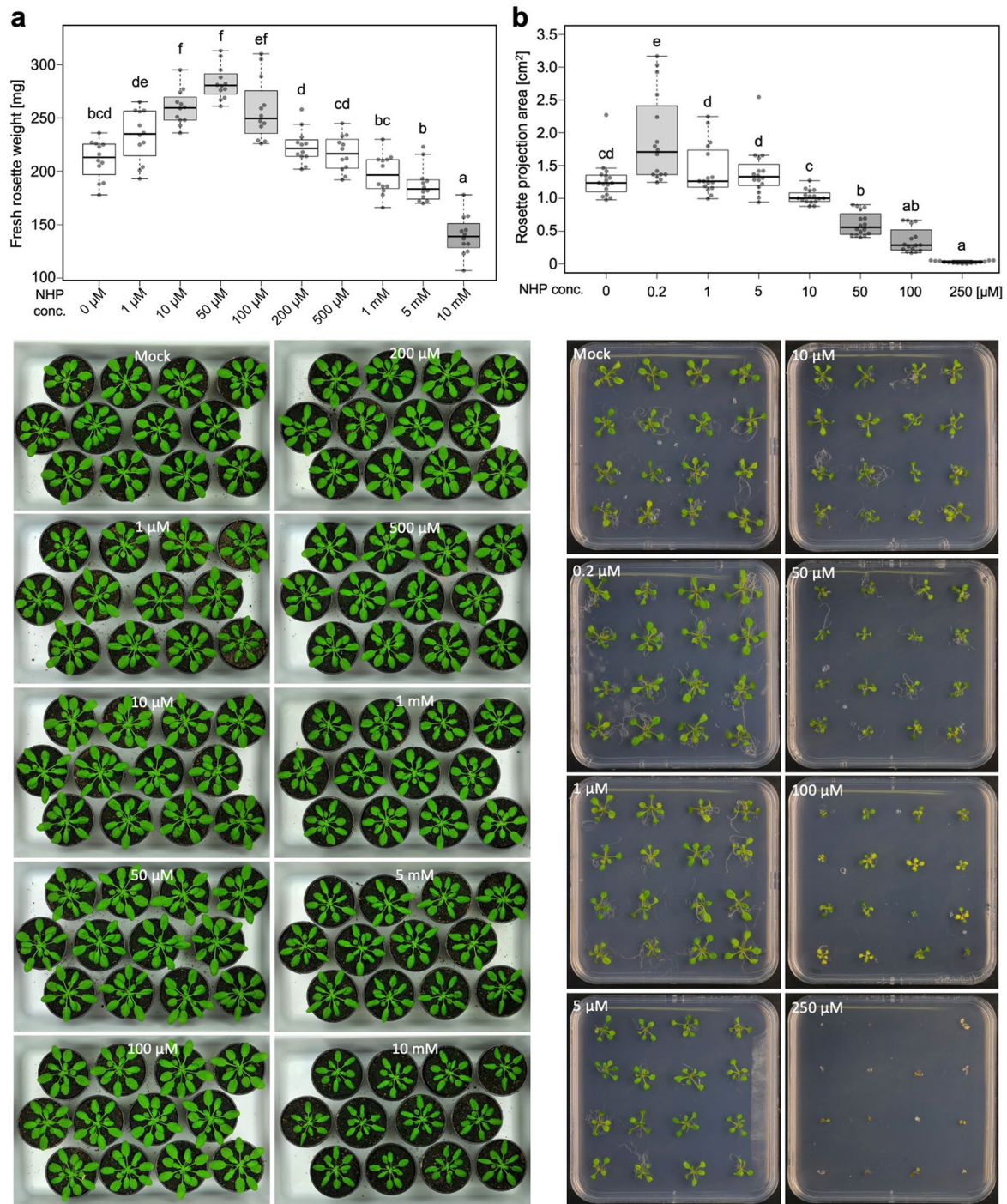
Bars represent means \pm standard error, $n = 4$. Root in grey and shoot in green. **b**, NHP and NHP-O-Gluc content in roots and shoots with or without *Ci* inoculation. Box in grey represent for root, white for shoot. Boxes represent the interquartile range (Q1–Q3), with the median shown as a bold line. Whiskers extend to $1.5 \times \text{IQR}$, $n = 4$; this analysis was performed once with four independent samples. Significant differences between mock and *Ci*-inoculated tissues were analyzed using the Welch two-sample t-test ($*p < 0.05$, $**p < 0.01$, $***p < 0.001$; n.s., not significant). The experiments (**a**, **b**) were conducted once with four independent biological replicates.



Extended Data Fig. 8 | Life span and active degradation of UGT76B1 protein.

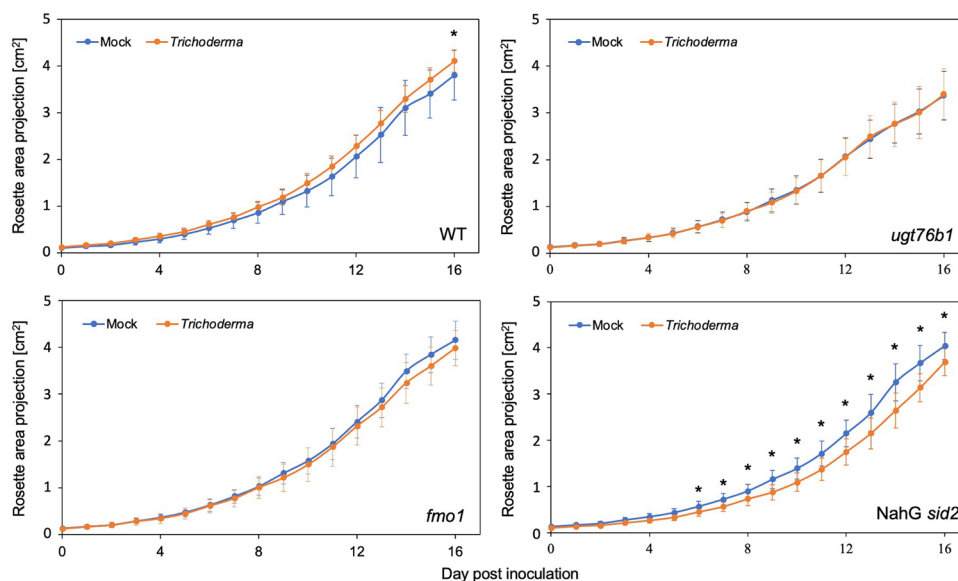
a, Longitudinal sections of a root from a two-week-old plant grown in hydroponic culture, with 100 μ M cycloheximide added to the medium to prevent protein synthesis. The mTFP-UGT76B1 signal remained strong in the root even after 3 days of treatment. Five days after the addition of the inhibitor, cell collapse began. Bar: 50 μ m. **b**, UGT76B1 is constitutively present in all layers of root cells

in the *ugt76b1.3SS_{pro}::mTFP-UGT76B1* overexpression line. Upon interaction with *Trichoderma*, the mTFP signal is lost in the outer root cell layers within 1 day, arguing for a rapid degradation of the *per se* stable protein (panel a). In contrast, some signal remains in the stele, where *T. harzianum* hyphae may not be able to penetrate. BF, bright field; PI, propidium iodide staining. Bar, 30 μ m. Both experiments were repeated twice with similar results.



Extended Data Fig. 9 | Dosage-dependent effect of NHP. a, WT plants grown on soil were watered with 2 ml of NHP at different concentrations twice a week. Fresh weights are measured after four weeks in parallel to the recording of projected leaf area (Fig. 5a). The comparison was performed once. Both analyses resulted in similar recording of plant growth. **b**, Plants were grown on half-strength MS plates supplemented with different concentrations of NHP. The rosette projection area of three-week-old plants was recorded. The results indicate that low concentrations of NHP stimulate plant growth, whereas high concentrations

inhibit it, with 250 μ M NHP being lethal on plates. Grey boxes indicate groups significantly different from the mock. Boxes represent the interquartile range (Q1–Q3), with the median shown as a bold line. Whiskers extend to $1.5 \times \text{IQR}$, $n = 16$. Significant differences were analyzed by one-way ANOVA with post-hoc Lincon test as indicated by letters. Leaf projection areas were measured using ImageJ. Both experiments were independently repeated twice with similar results.



Extended Data Fig. 10 | Growth promotion by *T. harzianum* is NHP- and SA-dependent. One-week-old plants were inoculated with 5 ml of a solution containing 10^6 conidia ml⁻¹. Leaf projection area was determined based on imaging regions with active chlorophyll fluorescence, measured daily at 6 a.m. Compared to mock treatment, inoculation with *Trichoderma* significantly enhanced growth of WT plants, an effect not observed for *fmo1* and *ugt76b1* mutants. In SA-depleted plants (*NahG sid2*), the growth response to *Trichoderma* inoculation was lost and even reverted. Alonso-Ramírez et al.⁵¹ have shown that *sid2* mutants are over-colonized by *T. harzianum*, it colonizes the vasculature and finally kills the plant. SA is important for the plant to keep *Trichoderma* in a beneficial rather than a pathogenic state (Poveda et al., 2023). *ugt76b1* has very high endogenous SA and NHP level (Bauer et al.³³), which may also prevent

Trichoderma from accessing the root. *ugt76b1* and *fmo1* both show abolished growth promotion by *Trichoderma*, which supports the notion that NHP is also critical for the interaction. Brotman et al.²³ showed an induction of *FMO1* transcripts in root upon *Trichoderma*. *fmo1* mutant is also stronger infested by *Trichoderma*. NHP seems as to be as important as SA in the interaction of both species. Thus, UGT76B1's activity towards NHP and SA may affect the interaction. However, the high SA level is dependent on MHP (FMO1) (Bauer et al.³³). n = 10, error bars represent standard deviation. Differences between mock and *Trichoderma* inoculation in each time point were analysed by Welch two-sample t test; *p < 0.05. The experiments were independently repeated twice with similar results.

Reporting Summary

Nature Portfolio wishes to improve the reproducibility of the work that we publish. This form provides structure for consistency and transparency in reporting. For further information on Nature Portfolio policies, see our [Editorial Policies](#) and the [Editorial Policy Checklist](#).

Statistics

For all statistical analyses, confirm that the following items are present in the figure legend, table legend, main text, or Methods section.

n/a	Confirmed
<input type="checkbox"/>	<input checked="" type="checkbox"/> The exact sample size (<i>n</i>) for each experimental group/condition, given as a discrete number and unit of measurement
<input type="checkbox"/>	<input checked="" type="checkbox"/> A statement on whether measurements were taken from distinct samples or whether the same sample was measured repeatedly
<input type="checkbox"/>	<input checked="" type="checkbox"/> The statistical test(s) used AND whether they are one- or two-sided <i>Only common tests should be described solely by name; describe more complex techniques in the Methods section.</i>
<input checked="" type="checkbox"/>	<input type="checkbox"/> A description of all covariates tested
<input type="checkbox"/>	<input checked="" type="checkbox"/> A description of any assumptions or corrections, such as tests of normality and adjustment for multiple comparisons
<input type="checkbox"/>	<input checked="" type="checkbox"/> A full description of the statistical parameters including central tendency (e.g. means) or other basic estimates (e.g. regression coefficient) AND variation (e.g. standard deviation) or associated estimates of uncertainty (e.g. confidence intervals)
<input type="checkbox"/>	<input checked="" type="checkbox"/> For null hypothesis testing, the test statistic (e.g. <i>F</i> , <i>t</i> , <i>r</i>) with confidence intervals, effect sizes, degrees of freedom and <i>P</i> value noted <i>Give P values as exact values whenever suitable.</i>
<input checked="" type="checkbox"/>	<input type="checkbox"/> For Bayesian analysis, information on the choice of priors and Markov chain Monte Carlo settings
<input checked="" type="checkbox"/>	<input type="checkbox"/> For hierarchical and complex designs, identification of the appropriate level for tests and full reporting of outcomes
<input checked="" type="checkbox"/>	<input type="checkbox"/> Estimates of effect sizes (e.g. Cohen's <i>d</i> , Pearson's <i>r</i>), indicating how they were calculated

Our web collection on [statistics for biologists](#) contains articles on many of the points above.

Software and code

Policy information about [availability of computer code](#)

Data collection	ImageJ for Mac, version 1.53K PSI Plantscreen Data Analyser for Windows, version 3.1.7.21 Leica LAS-X for Windows, version 4.13 Bruker dataanalysis for Windows, version 4.2 Bruker quantanalysis for Windows, version 2.2
Data analysis	R studio for Mac, version 2024.09.1+394 R for Mac, version 4.4.1

For manuscripts utilizing custom algorithms or software that are central to the research but not yet described in published literature, software must be made available to editors and reviewers. We strongly encourage code deposition in a community repository (e.g. GitHub). See the Nature Portfolio [guidelines for submitting code & software](#) for further information.

Data

Policy information about [availability of data](#)

All manuscripts must include a [data availability statement](#). This statement should provide the following information, where applicable:

- Accession codes, unique identifiers, or web links for publicly available datasets
- A description of any restrictions on data availability
- For clinical datasets or third party data, please ensure that the statement adheres to our [policy](#)

All original data are compiled in the attached Excel file Xu_etal_OrigDataStatistics.xlsx

Research involving human participants, their data, or biological material

Policy information about studies with [human participants or human data](#). See also policy information about [sex, gender \(identity/presentation\), and sexual orientation](#) and [race, ethnicity and racism](#).

Reporting on sex and gender

Use the terms *sex* (biological attribute) and *gender* (shaped by social and cultural circumstances) carefully in order to avoid confusing both terms. Indicate if findings apply to only one sex or gender; describe whether sex and gender were considered in study design; whether sex and/or gender was determined based on self-reporting or assigned and methods used. Provide in the source data disaggregated sex and gender data, where this information has been collected, and if consent has been obtained for sharing of individual-level data; provide overall numbers in this Reporting Summary. Please state if this information has not been collected. Report sex- and gender-based analyses where performed, justify reasons for lack of sex- and gender-based analysis.

Reporting on race, ethnicity, or other socially relevant groupings

Please specify the socially constructed or socially relevant categorization variable(s) used in your manuscript and explain why they were used. Please note that such variables should not be used as proxies for other socially constructed/relevant variables (for example, race or ethnicity should not be used as a proxy for socioeconomic status). Provide clear definitions of the relevant terms used, how they were provided (by the participants/respondents, the researchers, or third parties), and the method(s) used to classify people into the different categories (e.g. self-report, census or administrative data, social media data, etc.) Please provide details about how you controlled for confounding variables in your analyses.

Population characteristics

Describe the covariate-relevant population characteristics of the human research participants (e.g. age, genotypic information, past and current diagnosis and treatment categories). If you filled out the behavioural & social sciences study design questions and have nothing to add here, write "See above."

Recruitment

Describe how participants were recruited. Outline any potential self-selection bias or other biases that may be present and how these are likely to impact results.

Ethics oversight

Identify the organization(s) that approved the study protocol.

Note that full information on the approval of the study protocol must also be provided in the manuscript.

Field-specific reporting

Please select the one below that is the best fit for your research. If you are not sure, read the appropriate sections before making your selection.

☒ Life sciences ☐ Behavioural & social sciences ☐ Ecological, evolutionary & environmental sciences

For a reference copy of the document with all sections, see [nature.com/documents/nr-reporting-summary-flat.pdf](https://www.nature.com/documents/nr-reporting-summary-flat.pdf)

Life sciences study design

All studies must disclose on these points even when the disclosure is negative.

Sample size

For the metabolic analysis, including Fig. 1c, Fig. 3c, Fig. 5b-c and Extended Data Fig. 7b all have a sample size of 4, Fig. 1b has a sample size of 3. The samples showed no significant deviation from a normal distribution. For RT-qPCR analysis and Pst disease assays, including Fig. 2, Fig. 3b, Extended Data Fig. 1 and Data Fig. 7a, a sample size of 4 was also employed. This aligns with standard practices in similar studies within this field, where a sample size of 4 is generally sufficient to yield reliable and reproducible results.

In plant rosette area measurements, the sample sizes varied depending on the experiment: 10 plants were used for Fig. 5e and Extended Data Fig. 10; 12 plants for Fig. 5a and Extended Data Fig. 4a and 9a; and 16 plants for Extended Data Fig. 9b. These plants were cultivated under an autonomous phenotyping system with well-controlled growth conditions, including substrate uniformity, light, watering, and humidity.

Data exclusions

No data were excluded.

Replication

All experiments in this study were repeated at least twice by the same individual. The Pst disease assay described in Fig. 3b was independently repeated twice each by Ping Xu and Sophia Fundneider, with consistent results across all repetitions. Confocal microscopy observations in Fig. 3a and Fig. 4 revealed identical phenomena independently observed by the same two individuals.

The supplementary experiment in Extended Data Fig. 1, derived from Fig. 2c, was conducted only once. However, as the results aligned with those in Fig. 2c, additional repetitions were not performed. In Fig. 5b-d, experiments involving the soil cultivation of Col and fmo1 mutant plants inoculated with different fungi were repeated multiple times with varying outcomes. In the initial trials, no phenotype or only subtle phenotypes were observed due to limitations in the fungal inoculation method. After modifying the method—by moistening the soil before inoculation and gently squeezing the pots to loosen the soil around the roots for better fungal conidia contact—three subsequent experiments yielded significant results in two trials, as shown in the figure. The third trial showed weaker significance but followed the same trend.

Fig. 2b-c: for this experiment it is very important to avoid and exclude plants with adventitious roots. If those were included, the grafting failed, gene expression and pathogen resistance may not significantly enhanced.

The NHP feeding experiments in Fig. 5a were performed in three times independently, while those in Extended Data Fig. 9b were conducted twice. Extended Data Fig. 9a represents an additional experiment performed in parallel with the third repetition of Fig. 5a, as suggested by reviewers. All replicates showed consistent results.

Experiment of Fig. 3c, Extended Fig. 7 only performed once. These experiments were conducted in response to a request from the reviewer during the peer review process, but were in line with other experiments of this work.

Randomization	<p>For plants grown in Petri dishes, including Fig. 1c, Fig. 2a-b, Fig. 3c and Extended Data Fig. 9, different genotypes were cultivated in the same Petri dish, with replicates taken from separate dishes. The position of each Petri dish was randomized periodically to minimize the effect of varying light conditions in different locations.</p> <p>For plants grown in the PSI phenotyping facility, different genotypes were interplanted in a staggered arrangement. Trays were periodically repositioned to mitigate batch effects and ensure uniform growth conditions.</p> <p>For plants grown in regular growth chambers, each pot was individually labeled, and plants were distributed randomly within the chamber. The entire tray was moved periodically to account for potential positional differences in light or environmental conditions.</p>
Blinding	<p>Blinding was not applied in this study. The data collected primarily involved quantitative measurements, such as metabolic profiling, gene expression analysis, and phenotypic evaluations, which were obtained using standardized instruments or protocols that minimize subjective bias. Moreover, the treatment groups and genotypes were inherently distinct and identifiable, making it impractical to implement blinding.</p>

Behavioural & social sciences study design

All studies must disclose on these points even when the disclosure is negative.

Study description	<i>Briefly describe the study type including whether data are quantitative, qualitative, or mixed-methods (e.g. qualitative cross-sectional, quantitative experimental, mixed-methods case study).</i>
Research sample	<i>State the research sample (e.g. Harvard university undergraduates, villagers in rural India) and provide relevant demographic information (e.g. age, sex) and indicate whether the sample is representative. Provide a rationale for the study sample chosen. For studies involving existing datasets, please describe the dataset and source.</i>
Sampling strategy	<i>Describe the sampling procedure (e.g. random, snowball, stratified, convenience). Describe the statistical methods that were used to predetermine sample size OR if no sample-size calculation was performed, describe how sample sizes were chosen and provide a rationale for why these sample sizes are sufficient. For qualitative data, please indicate whether data saturation was considered, and what criteria were used to decide that no further sampling was needed.</i>
Data collection	<i>Provide details about the data collection procedure, including the instruments or devices used to record the data (e.g. pen and paper, computer, eye tracker, video or audio equipment) whether anyone was present besides the participant(s) and the researcher, and whether the researcher was blind to experimental condition and/or the study hypothesis during data collection.</i>
Timing	<i>Indicate the start and stop dates of data collection. If there is a gap between collection periods, state the dates for each sample cohort.</i>
Data exclusions	<i>If no data were excluded from the analyses, state so OR if data were excluded, provide the exact number of exclusions and the rationale behind them, indicating whether exclusion criteria were pre-established.</i>
Non-participation	<i>State how many participants dropped out/declined participation and the reason(s) given OR provide response rate OR state that no participants dropped out/declined participation.</i>
Randomization	<i>If participants were not allocated into experimental groups, state so OR describe how participants were allocated to groups, and if allocation was not random, describe how covariates were controlled.</i>

Ecological, evolutionary & environmental sciences study design

All studies must disclose on these points even when the disclosure is negative.

Study description	<i>Briefly describe the study. For quantitative data include treatment factors and interactions, design structure (e.g. factorial, nested, hierarchical), nature and number of experimental units and replicates.</i>
-------------------	---

Research sample	<i>Describe the research sample (e.g. a group of tagged <i>Passer domesticus</i>, all <i>Stenocereus thurberi</i> within Organ Pipe Cactus National Monument), and provide a rationale for the sample choice. When relevant, describe the organism taxa, source, sex, age range and any manipulations. State what population the sample is meant to represent when applicable. For studies involving existing datasets, describe the data and its source.</i>
Sampling strategy	<i>Note the sampling procedure. Describe the statistical methods that were used to predetermine sample size OR if no sample-size calculation was performed, describe how sample sizes were chosen and provide a rationale for why these sample sizes are sufficient.</i>
Data collection	<i>Describe the data collection procedure, including who recorded the data and how.</i>
Timing and spatial scale	<i>Indicate the start and stop dates of data collection, noting the frequency and periodicity of sampling and providing a rationale for these choices. If there is a gap between collection periods, state the dates for each sample cohort. Specify the spatial scale from which the data are taken</i>
Data exclusions	<i>If no data were excluded from the analyses, state so OR if data were excluded, describe the exclusions and the rationale behind them, indicating whether exclusion criteria were pre-established.</i>
Reproducibility	<i>Describe the measures taken to verify the reproducibility of experimental findings. For each experiment, note whether any attempts to repeat the experiment failed OR state that all attempts to repeat the experiment were successful.</i>
Randomization	<i>Describe how samples/organisms/participants were allocated into groups. If allocation was not random, describe how covariates were controlled. If this is not relevant to your study, explain why.</i>
Blinding	<i>Describe the extent of blinding used during data acquisition and analysis. If blinding was not possible, describe why OR explain why blinding was not relevant to your study.</i>

Did the study involve field work? ☐ Yes ☒ No

Field work, collection and transport

Field conditions	<i>Describe the study conditions for field work, providing relevant parameters (e.g. temperature, rainfall).</i>
Location	<i>State the location of the sampling or experiment, providing relevant parameters (e.g. latitude and longitude, elevation, water depth).</i>
Access & import/export	<i>Describe the efforts you have made to access habitats and to collect and import/export your samples in a responsible manner and in compliance with local, national and international laws, noting any permits that were obtained (give the name of the issuing authority, the date of issue, and any identifying information).</i>
Disturbance	<i>Describe any disturbance caused by the study and how it was minimized.</i>

Reporting for specific materials, systems and methods

We require information from authors about some types of materials, experimental systems and methods used in many studies. Here, indicate whether each material, system or method listed is relevant to your study. If you are not sure if a list item applies to your research, read the appropriate section before selecting a response.

Materials & experimental systems

n/a	Involved in the study
<input checked="" type="checkbox"/>	<input type="checkbox"/> Antibodies
<input checked="" type="checkbox"/>	<input type="checkbox"/> Eukaryotic cell lines
<input checked="" type="checkbox"/>	<input type="checkbox"/> Palaeontology and archaeology
<input checked="" type="checkbox"/>	<input type="checkbox"/> Animals and other organisms
<input checked="" type="checkbox"/>	<input type="checkbox"/> Clinical data
<input checked="" type="checkbox"/>	<input type="checkbox"/> Dual use research of concern
<input type="checkbox"/>	<input checked="" type="checkbox"/> Plants

Methods

n/a	Involved in the study
<input checked="" type="checkbox"/>	<input type="checkbox"/> ChIP-seq
<input checked="" type="checkbox"/>	<input type="checkbox"/> Flow cytometry
<input checked="" type="checkbox"/>	<input type="checkbox"/> MRI-based neuroimaging

Antibodies

Antibodies used	<i>Describe all antibodies used in the study; as applicable, provide supplier name, catalog number, clone name, and lot number.</i>
Validation	<i>Describe the validation of each primary antibody for the species and application, noting any validation statements on the manufacturer's website, relevant citations, antibody profiles in online databases, or data provided in the manuscript.</i>

Eukaryotic cell lines

Policy information about [cell lines and Sex and Gender in Research](#)

Cell line source(s)	State the source of each cell line used and the sex of all primary cell lines and cells derived from human participants or vertebrate models.
Authentication	Describe the authentication procedures for each cell line used OR declare that none of the cell lines used were authenticated.
Mycoplasma contamination	Confirm that all cell lines tested negative for mycoplasma contamination OR describe the results of the testing for mycoplasma contamination OR declare that the cell lines were not tested for mycoplasma contamination.
Commonly misidentified lines (See ICLAC register)	Name any commonly misidentified cell lines used in the study and provide a rationale for their use.

Palaeontology and Archaeology

Specimen provenance	Provide provenance information for specimens and describe permits that were obtained for the work (including the name of the issuing authority, the date of issue, and any identifying information). Permits should encompass collection and, where applicable, export.
Specimen deposition	Indicate where the specimens have been deposited to permit free access by other researchers.
Dating methods	If new dates are provided, describe how they were obtained (e.g. collection, storage, sample pretreatment and measurement), where they were obtained (i.e. lab name), the calibration program and the protocol for quality assurance OR state that no new dates are provided.
<input type="checkbox"/> Tick this box to confirm that the raw and calibrated dates are available in the paper or in Supplementary Information.	
Ethics oversight	Identify the organization(s) that approved or provided guidance on the study protocol, OR state that no ethical approval or guidance was required and explain why not.

Note that full information on the approval of the study protocol must also be provided in the manuscript.

Animals and other research organisms

Policy information about [studies involving animals; ARRIVE guidelines](#) recommended for reporting animal research, and [Sex and Gender in Research](#)

Laboratory animals	For laboratory animals, report species, strain and age OR state that the study did not involve laboratory animals.
Wild animals	Provide details on animals observed in or captured in the field; report species and age where possible. Describe how animals were caught and transported and what happened to captive animals after the study (if killed, explain why and describe method; if released, say where and when) OR state that the study did not involve wild animals.
Reporting on sex	Indicate if findings apply to only one sex; describe whether sex was considered in study design, methods used for assigning sex. Provide data disaggregated for sex where this information has been collected in the source data as appropriate; provide overall numbers in this Reporting Summary. Please state if this information has not been collected. Report sex-based analyses where performed, justify reasons for lack of sex-based analysis.
Field-collected samples	For laboratory work with field-collected samples, describe all relevant parameters such as housing, maintenance, temperature, photoperiod and end-of-experiment protocol OR state that the study did not involve samples collected from the field.
Ethics oversight	Identify the organization(s) that approved or provided guidance on the study protocol, OR state that no ethical approval or guidance was required and explain why not.

Note that full information on the approval of the study protocol must also be provided in the manuscript.

Clinical data

Policy information about [clinical studies](#)

All manuscripts must comply with the ICMJE [guidelines for publication of clinical research](#) and a completed [CONSORT checklist](#) must be included with all submissions.

Clinical trial registration	Provide the trial registration number from ClinicalTrials.gov or an equivalent agency.
Study protocol	Note where the full trial protocol can be accessed OR if not available, explain why.
Data collection	Describe the settings and locales of data collection, noting the time periods of recruitment and data collection.

Dual use research of concern

Policy information about [dual use research of concern](#)

Hazards

Could the accidental, deliberate or reckless misuse of agents or technologies generated in the work, or the application of information presented in the manuscript, pose a threat to:

No	Yes
<input checked="" type="checkbox"/>	<input type="checkbox"/> Public health
<input checked="" type="checkbox"/>	<input type="checkbox"/> National security
<input checked="" type="checkbox"/>	<input type="checkbox"/> Crops and/or livestock
<input checked="" type="checkbox"/>	<input type="checkbox"/> Ecosystems
<input checked="" type="checkbox"/>	<input type="checkbox"/> Any other significant area

Experiments of concern

Does the work involve any of these experiments of concern:

No	Yes
<input checked="" type="checkbox"/>	<input type="checkbox"/> Demonstrate how to render a vaccine ineffective
<input checked="" type="checkbox"/>	<input type="checkbox"/> Confer resistance to therapeutically useful antibiotics or antiviral agents
<input checked="" type="checkbox"/>	<input type="checkbox"/> Enhance the virulence of a pathogen or render a nonpathogen virulent
<input checked="" type="checkbox"/>	<input type="checkbox"/> Increase transmissibility of a pathogen
<input checked="" type="checkbox"/>	<input type="checkbox"/> Alter the host range of a pathogen
<input checked="" type="checkbox"/>	<input type="checkbox"/> Enable evasion of diagnostic/detection modalities
<input checked="" type="checkbox"/>	<input type="checkbox"/> Enable the weaponization of a biological agent or toxin
<input checked="" type="checkbox"/>	<input type="checkbox"/> Any other potentially harmful combination of experiments and agents

Plants

Seed stocks	All details are included in the methods part of the manuscripts.
Novel plant genotypes	All details are included in the methods part of the manuscripts.
Authentication	<p>PCR-based genotyping was conducted to confirm the presence and homozygosity of the <i>ugt76b1</i> and <i>fmo1</i> insertion mutants following the protocol described at http://signal.salk.edu/tdnaprimers.2.html. The point mutation resulting to a stop codon in <i>sid2</i></p> <p>For the mTFP-UGT76B1 complementation lines and tissue-specific knockout lines, fluorescent signals from the seed coat were utilized to identify transgenic plants. The selected plants were further verified using confocal microscopy to confirm their expected features. Additionally, segregation ratios were recorded to ensure a single T-DNA insertion event in these lines.</p>

ChIP-seq

Data deposition

- ☐ Confirm that both raw and final processed data have been deposited in a public database such as [GEO](#).
- ☐ Confirm that you have deposited or provided access to graph files (e.g. BED files) for the called peaks.

Data access links

May remain private before publication.

For "Initial submission" or "Revised version" documents, provide reviewer access links. For your "Final submission" document, provide a link to the deposited data.

Files in database submission

Provide a list of all files available in the database submission.

Genome browser session (e.g. [UCSC](#))

Provide a link to an anonymized genome browser session for "Initial submission" and "Revised version" documents only, to enable peer review. Write "no longer applicable" for "Final submission" documents.

Methodology

Replicates	Describe the experimental replicates, specifying number, type and replicate agreement.
Sequencing depth	Describe the sequencing depth for each experiment, providing the total number of reads, uniquely mapped reads, length of reads and whether they were paired- or single-end.
Antibodies	Describe the antibodies used for the ChIP-seq experiments; as applicable, provide supplier name, catalog number, clone name, and lot number.
Peak calling parameters	Specify the command line program and parameters used for read mapping and peak calling, including the ChIP, control and index files used.
Data quality	Describe the methods used to ensure data quality in full detail, including how many peaks are at FDR 5% and above 5-fold enrichment.
Software	Describe the software used to collect and analyze the ChIP-seq data. For custom code that has been deposited into a community repository, provide accession details.

Flow Cytometry

Plots

Confirm that:

- ☐ The axis labels state the marker and fluorochrome used (e.g. CD4-FITC).
- ☐ The axis scales are clearly visible. Include numbers along axes only for bottom left plot of group (a 'group' is an analysis of identical markers).
- ☐ All plots are contour plots with outliers or pseudocolor plots.
- ☐ A numerical value for number of cells or percentage (with statistics) is provided.

Methodology

Sample preparation	Describe the sample preparation, detailing the biological source of the cells and any tissue processing steps used.
Instrument	Identify the instrument used for data collection, specifying make and model number.
Software	Describe the software used to collect and analyze the flow cytometry data. For custom code that has been deposited into a community repository, provide accession details.
Cell population abundance	Describe the abundance of the relevant cell populations within post-sort fractions, providing details on the purity of the samples and how it was determined.
Gating strategy	Describe the gating strategy used for all relevant experiments, specifying the preliminary FSC/SSC gates of the starting cell population, indicating where boundaries between "positive" and "negative" staining cell populations are defined.
<input type="checkbox"/> Tick this box to confirm that a figure exemplifying the gating strategy is provided in the Supplementary Information.	

Magnetic resonance imaging

Experimental design

Design type	Indicate task or resting state; event-related or block design.
Design specifications	Specify the number of blocks, trials or experimental units per session and/or subject, and specify the length of each trial or block (if trials are blocked) and interval between trials.
Behavioral performance measures	State number and/or type of variables recorded (e.g. correct button press, response time) and what statistics were used to establish that the subjects were performing the task as expected (e.g. mean, range, and/or standard deviation across subjects).

Acquisition

Imaging type(s)	<i>Specify: functional, structural, diffusion, perfusion.</i>
Field strength	<i>Specify in Tesla</i>
Sequence & imaging parameters	<i>Specify the pulse sequence type (gradient echo, spin echo, etc.), imaging type (EPI, spiral, etc.), field of view, matrix size, slice thickness, orientation and TE/TR/flip angle.</i>
Area of acquisition	<i>State whether a whole brain scan was used OR define the area of acquisition, describing how the region was determined.</i>
Diffusion MRI	<input type="checkbox"/> Used <input type="checkbox"/> Not used

Preprocessing

Preprocessing software	<i>Provide detail on software version and revision number and on specific parameters (model/functions, brain extraction, segmentation, smoothing kernel size, etc.).</i>
Normalization	<i>If data were normalized/standardized, describe the approach(es): specify linear or non-linear and define image types used for transformation OR indicate that data were not normalized and explain rationale for lack of normalization.</i>
Normalization template	<i>Describe the template used for normalization/transformation, specifying subject space or group standardized space (e.g. original Talairach, MNI305, ICBM152) OR indicate that the data were not normalized.</i>
Noise and artifact removal	<i>Describe your procedure(s) for artifact and structured noise removal, specifying motion parameters, tissue signals and physiological signals (heart rate, respiration).</i>
Volume censoring	<i>Define your software and/or method and criteria for volume censoring, and state the extent of such censoring.</i>

Statistical modeling & inference

Model type and settings	<i>Specify type (mass univariate, multivariate, RSA, predictive, etc.) and describe essential details of the model at the first and second levels (e.g. fixed, random or mixed effects; drift or auto-correlation).</i>
Effect(s) tested	<i>Define precise effect in terms of the task or stimulus conditions instead of psychological concepts and indicate whether ANOVA or factorial designs were used.</i>
Specify type of analysis:	<input type="checkbox"/> Whole brain <input type="checkbox"/> ROI-based <input type="checkbox"/> Both
Statistic type for inference	<i>Specify voxel-wise or cluster-wise and report all relevant parameters for cluster-wise methods.</i>
(See Eklund et al. 2016)	
Correction	<i>Describe the type of correction and how it is obtained for multiple comparisons (e.g. FWE, FDR, permutation or Monte Carlo).</i>

Models & analysis

n/a	Involvement in the study
<input type="checkbox"/>	<input type="checkbox"/> Functional and/or effective connectivity
<input type="checkbox"/>	<input type="checkbox"/> Graph analysis
<input type="checkbox"/>	<input type="checkbox"/> Multivariate modeling or predictive analysis
Functional and/or effective connectivity	<i>Report the measures of dependence used and the model details (e.g. Pearson correlation, partial correlation, mutual information).</i>
Graph analysis	<i>Report the dependent variable and connectivity measure, specifying weighted graph or binarized graph, subject- or group-level, and the global and/or node summaries used (e.g. clustering coefficient, efficiency, etc.).</i>
Multivariate modeling and predictive analysis	<i>Specify independent variables, features extraction and dimension reduction, model, training and evaluation metrics.</i>